

Analytical approaches to time and length scales in models of glasses

Silvio Franz

Université Paris Sud, CNRS, LPTMS, UMR8626, Orsay F-91405, France

Guilhem Semerjian

LPTENS, Unité Mixte de Recherche (UMR 8549) du CNRS et de l'ENS associée à l'université Pierre et Marie Curie, 24 Rue Lhomond, 75231 Paris Cedex 05, France.

OXFORD
UNIVERSITY PRESS

Abstract

The goal of this chapter is to review recent analytical results about the growth of a (static) correlation length in glassy systems, and the connection that can be made between this length scale and the equilibrium correlation time of its dynamics. The definition of such a length scale is first given in a generic setting, including finite-dimensional models, along with rigorous bounds linking it to the correlation time. We then present some particular cases (finite connectivity mean-field models, and Kac limit of finite dimensional systems) where this length can be actually computed.

0.1 Introduction

The “Random first order theory” (RFOT) is one of the most widely discussed theory of glass formation and glassy phenomena in fragile systems. Its origin is based upon the observation by Kirkpatrick, Wolynes and Thirumalai (1) that a family of abstract long range spin glass models with “one step replica symmetry breaking” (1RSB) (2) presents freezing phenomena that in several aspects resemble the observed phenomenology in freezing of fragile liquids and other glassy systems. In this perspective long range spin glasses provide a unifying description of glassy phenomena, including dynamical aspects (MCT dynamical singularity and aging phenomena) and thermodynamical ones (metastability and Kauzmann like entropy crisis), which have given rise to predictions verified in simulations and experiments (3; 4). Despite the appeal of the resulting picture, it immediately became clear that two problems had to be overcome to be able to apply convincingly the theory to supercooled liquids: 1) The disordered interactions of spin glasses models is not a realistic microscopic description of liquid systems 2) The 1RSB picture is strongly dependent on the long range character of the interactions and presents some typical pathologies of mean-field theories. Both problems have attracted a lot of attention.

The first problem has been basically circumvented by the fact that the most sophisticated Mean-Field theories based on realistic liquid models of particles in interaction give back the 1RSB scenario (5). This suggests a high level of universality of glassy phenomena that goes from spin models with random interactions to supercooled liquids, one can thus expect to understand general properties of the latter ones from the study of the former ones, which are simpler microscopically.

The second problem, that is how to effectively take into account the finite range character of the interactions, remains in our opinion the main obstacle against an accomplished theory of the glass transition, despite important contributions. The RFOT, based on scaling and phenomenological arguments, proposes an intriguing scenario about which features of Mean-Field Theory survive in short range systems and what of the picture should be modified. However, a theory based on a first principle analysis of microscopic models is unfortunately lacking. Understanding the role of finite-range

interactions includes both important questions of principle, but not directly related to physical observables such as the possibility of an ideal glass transition in systems with short range interactions, and questions of direct practical interest as finding a theory for activated dynamics and the cross-over between mode coupling behavior and activation.

This chapter reviews some of the theoretical efforts to understand the relation between the physics of finite dimensional glassy systems and their mean field description and to include finite range interactions in microscopic models of glassy phenomena. A crucial point that an accomplished theory of the glass transition should address is the growth of correlations that accompanies the increase of relaxation time as temperature is decreased. The relaxation time of a supercooled liquid increases dramatically upon lowering its temperature, until reaching experimentally accessible timescales at the laboratory glass transition temperature T_g . In this range of temperature the usual static spatial correlations (for instance the structure factor measured in scattering experiments) remain essentially the same as the ones of a high temperature liquid. These two facts seem contradictory: the physical intuition relates a large correlation time to cooperative relaxation mechanisms involving a large volume of the sample (which incidentally is an argument in favour of the universality of glassy phenomena, the microscopic details being “averaged out” in this case), hence the very strong increase of the relaxation time around T_g should have a trace in spatial correlations. One way to address this puzzle is to define dynamical correlation lengths. Convincing experiments (4), following numerical simulations (6) and dynamical theories (7; 8) have, after a long search, demonstrated for the first time growing dynamical correlations (7; 8; 4). Another way, which we shall review in this contribution, is to define a static correlation length through a point-to-set procedure slightly more involved than the two-point function underlying the definition of the structure factor.

A large part of this chapter will be devoted to the discussion of this length and its relation with the relaxation time. In Sec. 0.2 we explain in details the definition of the point-to-set correlation length and we show how it allows to prove bounds between this correlation length and the equilibrium correlation time that agrees with the intuition sketched above. We then discuss two classes of disordered spin models of the 1RSB type where spatial aspects can be addressed through analytic techniques, namely models on diluted random graphs and finite dimensional models in the Kac limit. In the first class of models, considered in Sec. 0.3, each spin interacts with a finite number of other spins chosen at random. These models can be solved exactly through the cavity method; in agreement with the general bounds, at the point of dynamical transition both the relaxation time and the correlation length are divergent. The second class, studied in Sec. 0.4, consists in genuine finite dimensional models with a tunable interaction range r_0 . In the limit of large r_0 one can compute the point-to-set correlation function and associated correlation lengths. This leads to a detailed picture of glassy phenomena, with a dynamical and static correlation lengths that do not necessarily coincide.

We hope the style of presentation adopted in this chapter will provide the reader with a global view and some mathematical and theoretical tools which should make easier the reading of the original, more formal, literature on the subjects we address.

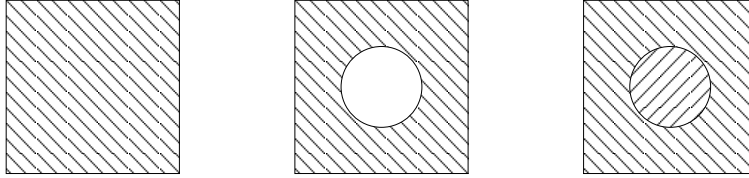


Fig. 0.1 Scheme of the thought experiment (9) underlying the definition of the point-to-set correlation length.

0.2 Definition of the point-to-set correlation function and its relation to correlation time

0.2.1 Heuristic discussion

In this section we want to introduce the notion of point-to-set correlation functions and to show that the correlation length derived from it is relevant for glassy systems, as upper and lower bounds on the correlation time can be inferred from this length. The presentation will be first done in an informal way, following the thought experiment first discussed in (9). We shall then revisit it with more mathematical definitions and sketch the results and the methods of proof of (10).

Let us consider the thought experiment of (9), schematized in Fig. 0.1. In a first time one takes a snapshot of an equilibrium configuration of the system under study, i.e. for instance the values of the spins, or the positions of particles depending on the model investigated. Let us call $\underline{\sigma}$ this first configuration, depicted on the first panel of Fig. 0.1. Suppose now that the configuration of the system is frozen to the value it has in $\underline{\sigma}$ outside a given volume \bar{B} around an arbitrary point, for instance the center of the system (see middle panel in Fig. 0.1), and that the interior is thermalized in presence of this boundary condition. One thus obtains another equilibrium configuration $\underline{\sigma}'$, which is forced to coincide with $\underline{\sigma}$ outside \bar{B} . Consider now the following question: how similar are $\underline{\sigma}$ and $\underline{\sigma}'$ around the center of the system? A precise notion of similarity shall be given below, in any case it is natural to expect that the larger the volume \bar{B} , the less similar should $\underline{\sigma}$ and $\underline{\sigma}'$ be at its center. Indeed the influence of the boundary conditions, which force $\underline{\sigma}'$ to be very close to $\underline{\sigma}$ when \bar{B} is small, becomes less and less efficient when the boundary is pushed away. This procedure thus allow to define a correlation function between a point (the center of the system) and a set of points (the boundary of \bar{B}), hence the name already mentioned. It is understood that in the correlation function the similarity measure should be averaged with respect to the configurations $\underline{\sigma}$ and $\underline{\sigma}'$. From this function one can further define a correlation length. Taking for simplicity \bar{B} to be a spherical ball of radius ℓ , we shall indeed define the correlation length ℓ_c as the minimal radius which brings the point-to-set correlation function (i.e. the average measure of similarity of the center of $\underline{\sigma}$ and $\underline{\sigma}'$) below a small threshold fixed beforehand.

The equilibrium correlation time τ_c of the system can be defined in a similar fashion, as the minimal time necessary for the auto-correlation function (average similarity measure at the same point, between one equilibrium configuration and the outcome of its evolution during a certain amount of time) to drop below a given threshold. It turns

out that the intuition discussed in the introduction, namely that large correlation times and large correlation lengths are two intertwined phenomena, can be given a precise content with these two definitions of τ_c and ℓ_c . Indeed the rigorous proof of (10) we shall sketch below implies that $\ell_c \leq \tau_c \leq \exp\{\ell_c^d\}$, where we have hidden for simplicity several constants. The interpretation of these two inequalities might sound disappointingly simple. As ℓ_c measures the radius of a correlated region of the system, and as for the center of the system to decorrelate it must receive some information from the boundary of the correlated region, the lower bound merely states that this information cannot propagate faster than ballistically. On the other hand the upper bound follows from the fact that the dynamics of the center of the system is weakly sensitive to the outside of the correlated zone, hence it should closely resemble the dynamics of the ball of radius ℓ_c without its surrounding environment. The latter case being the dynamics of a finite system of volume ℓ_c^d (where d denotes the dimension of the system), its relaxation cannot be slower than exponential in its volume.

The fact that these two inequalities have natural interpretations does not mean they have a trivial content, but rather demonstrates the relevance of the point-to-set definition of the correlation length ℓ_c . Recall indeed that one of the puzzle of the glass phenomenology is the drastic growth of the relaxation time without significant traces in the structure factor, hence in the 2-point correlation length. The bounds between τ_c and ℓ_c show that despite this fact the growth of the relaxation time must be accompanied by a growth of a (static) correlation length if the latter is appropriately defined.

0.2.2 More precise definition of the correlation function

We want now to provide the reader with more formal definitions of the quantities discussed informally above, before restating with more details the bounds between the correlation length and the correlation time. Note that if point-to-set correlations are relatively new in physics they are quite common in the mathematical literature, in particular in the context of the so-called tree reconstruction problem, see for instance (12; 11).

For the sake of concreteness we shall consider a model of N Ising spins $\sigma_i = \pm 1$, whose global configuration will be denoted $\underline{\sigma} = (\sigma_1, \dots, \sigma_N)$. For a subset S of the variable indexes $\{1, \dots, N\}$ we will call $\underline{\sigma}_S$ the configuration of the variables in S . The energy function (Hamiltonian) is decomposed as $E(\underline{\sigma}) = \sum_{a=1}^M E_a(\underline{\sigma}_{\partial a})$, that is a sum of M terms E_a , with the a -th term involving a subset denoted ∂a of the variables. For instance in a two dimensional square lattice model with nearest neighbor interactions there would be an interaction a for each edge of the lattice. The definition of E encompasses however more general cases, in particular multi-spin interactions involving more than a pair of spins. It can be convenient in such a case to represent the network of interactions as a so-called factor graph (13), see Figure 0.2 for an illustration. Each variable $\sigma_1, \dots, \sigma_N$ is associated to a circle vertex, while the interactions E_1, \dots, E_M are symbolized with square vertices. An edge is drawn between a variable i and an interaction a if and only if E_a depends on σ_i . On the right panel of Fig. 0.2 is drawn a portion of the factor graph corresponding to a square lattice model.

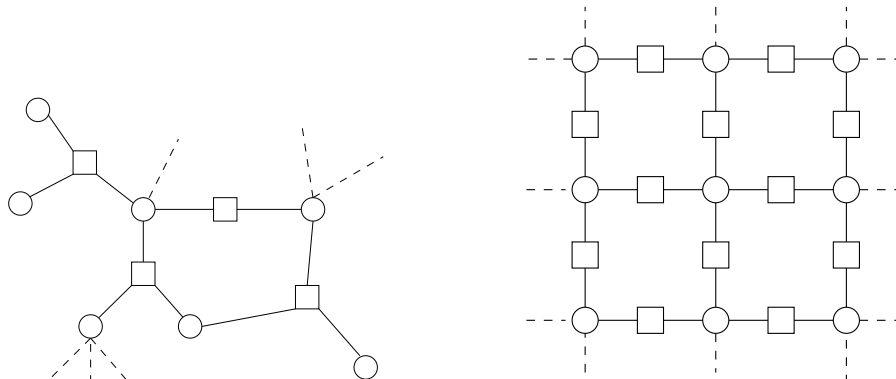


Fig. 0.2 Left: general example of a factor graph representing an energy $E(\underline{\sigma}) = \sum_{a=1}^M E_a(\underline{\sigma}_{\partial a})$. Each circle represents a variable σ_i , each square an interaction term E_a . An edge is drawn between E_a and σ_i whenever the a -th interaction depends on the i -th variable. Right: the case of a square lattice with nearest neighbor interactions.

We will use in the following the notation $d(i, j)$ for the distance between two variables. This will be taken as the graphical distance on the factor graph, that is the number of interactions that have to be crossed along a shortest path linking i and j . This notion of distance has the virtue of being well-defined for any topology of the interaction network, not only for finite-dimensional models. In the latter case the graph distance is equivalent to the Euclidean one.

The Gibbs-Boltzmann probability measure is defined on the space of configurations by $\mu(\underline{\sigma}) = \exp[-\beta E(\underline{\sigma})]/Z$, with the partition function Z ensuring its normalization. Angular brackets $\langle \cdot \rangle$ will be used to denote averages with respect to this law. In order to quantify the amount of correlations induced by the Gibbs-Boltzmann probability between one variable, say σ_i , and a set B of other variables, one can consider a function $F(\underline{\sigma}_B)$ which depends only on the values of the variables in B , and compute the correlation between the two as $\langle \sigma_i F(\underline{\sigma}_B) \rangle - \langle \sigma_i \rangle \langle F(\underline{\sigma}_B) \rangle$. If for instance σ_i were completely independent from the status of the variables in B this quantity would vanish. To make contact with the thought experiment explained above one can choose as a particular function F the magnetization of the i -th spin *conditioned* on $\underline{\sigma}_B$, denoted $\langle \sigma_i \rangle_{\underline{\sigma}_B}$. This conditional average is defined for an arbitrary function f as

$$\langle f(\underline{\sigma}') \rangle_{\underline{\sigma}_B} = \sum_{\underline{\sigma}'} f(\underline{\sigma}') \mu(\underline{\sigma}' | \underline{\sigma}_B), \quad (0.1)$$

where the conditional probability is restricted to configurations which coincide with $\underline{\sigma}_B$ on the variables in B ,

$$\mu(\underline{\sigma}' | \underline{\sigma}_B) = \begin{cases} \frac{1}{Z(\underline{\sigma}_B)} e^{-\beta E(\underline{\sigma}')} & \text{if } \underline{\sigma}'_B = \underline{\sigma}_B \\ 0 & \text{otherwise} \end{cases}, \quad (0.2)$$

$Z(\underline{\sigma}_B)$ ensuring its normalization. With this choice for F we have thus obtained the correlation function between a point i and a set B as

x *Abstract*

$$G(i, B) = \langle \sigma_i \langle \sigma'_i \rangle_{\underline{\sigma}_B} \rangle - \langle \sigma_i \rangle^2 = \sum_{\underline{\sigma}} \mu(\underline{\sigma}) \sum_{\underline{\sigma}'} \mu(\underline{\sigma}' | \underline{\sigma}_B) \sigma_i \sigma'_i - \langle \sigma_i \rangle^2, \quad (0.3)$$

where the last expression enlightens the connection with the heuristic discussion above: the configuration $\underline{\sigma}'$ corresponds to the second equilibrium configuration drawn conditioned on the value in B of the first configuration $\underline{\sigma}$.

We would like to emphasize that the configuration $\underline{\sigma}'$ constructed in the second place is as representative as $\underline{\sigma}$ of the Gibbs-Boltzmann equilibrium measure, in other words for any function f of the configuration one has (14)

$$\langle \langle f(\underline{\sigma}') \rangle_{\underline{\sigma}_B} \rangle = \langle f(\underline{\sigma}) \rangle. \quad (0.4)$$

This property follows simply from the properties of conditional probability and its proof will be omitted. In the following sections we will consider correlations between replicas of the system with the same constraint (i.e. $\underline{\sigma}'$ and $\underline{\sigma}''$ are generated independently from $\mu(\cdot | \underline{\sigma}_B)$ for fixed $\underline{\sigma}_B$ and quenched disorder in the energy function E). Given any two functions $f(\underline{\sigma})$ and $g(\underline{\sigma})$ one can define the correlation

$$C(f, g) = \langle \langle f(\underline{\sigma}') \rangle_{\underline{\sigma}_B} \langle g(\underline{\sigma}'') \rangle_{\underline{\sigma}_B} \rangle. \quad (0.5)$$

Similarly to (0.4) one can show that this coincides with the correlation between $\underline{\sigma}'$ and $\underline{\sigma}$ according to

$$C(f, g) = \langle f(\underline{\sigma}) \langle g(\underline{\sigma}') \rangle_{\underline{\sigma}_B} \rangle. \quad (0.6)$$

This identity will play an important role in the analysis of the point-to-set function in the Kac limit discussed in Sec. 0.4, and we shall call it conditional equilibrium condition.

We come back now to the definition of the point-to-set correlation function, and consider more specifically the case where B is the outside of a ball of radius ℓ around i , i.e. the set of variables at distance larger or equal than ℓ from variable i , $B(i, \ell) = \{j | d(i, j) \geq \ell\}$. We shall call $G(i, \ell) = G(i, B(i, \ell))$ the correlation function for this geometry. It is intuitively clear that $G(i, \ell)$ decreases when the radius ℓ of the ball increases, as farther away sites are less correlated with i . One can thus set a small threshold ε and defines the correlation length for site i as the minimal distance ℓ necessary to make the correlation $G(i, \ell)$ drops below the threshold ε . In formula, $\ell_i(\varepsilon) = \min\{\ell | G(i, \ell) \leq \varepsilon\}$.

We turn finally to the definition of the correlation time. We shall consider a single spin flip dynamics in continuous time, defined through transition rates $W(\underline{\sigma} \rightarrow \underline{\sigma}')$. The single spin flip assumption means that these rates vanish whenever $\underline{\sigma}$ and $\underline{\sigma}'$ differ in more than one variable. We assume the rates to verify the detailed balance condition

$$\mu(\underline{\sigma}) W(\underline{\sigma} \rightarrow \underline{\sigma}') = \mu(\underline{\sigma}') W(\underline{\sigma}' \rightarrow \underline{\sigma}), \quad (0.7)$$

which ensures that the Gibbs-Boltzmann probability is stationary under this dynamics. Moreover the rate from a configuration $\underline{\sigma}$ to the configuration where a single variable i has been flipped is assumed to depend on $\underline{\sigma}$ only through the configuration of σ_i and

of the variables at unit distance from i . This last condition is obviously fulfilled by the usual Monte Carlo dynamics like the Metropolis or heat-bath (Glauber) rules. The equilibrium dynamics of the model is defined by these rates and the initial condition $\underline{\sigma}(t=0)$ which is drawn from the equilibrium law μ . The average over the initial condition and the subsequent evolution shall be denoted again by angular brackets $\langle \dots \rangle$. The auto-correlation function of variable i is hence defined as $C_i(t) = \langle \sigma_i(0)\sigma_i(t) \rangle - \langle \sigma_i \rangle^2$, and we can assign a correlation time τ_i to this variable as $\tau_i(\varepsilon) = \min\{t | C_i(t) \leq \varepsilon\}$, i.e. as the minimal time for the auto-correlation function to drop below a given threshold ε . To avoid confusion in the following let us emphasize that in the definition of the correlation time we consider the dynamics of the *whole* system; the constraints on the finite ball B only appear in the definition of the correlation length.

0.2.3 Relation between the correlation length and the equilibrium correlation time

Now that the definitions of the correlation time τ_i and correlation length ℓ_i have been given more precisely we can restate in a more accurate way the bounds derived rigorously in (10):

$$C_1 \ell_i(\varepsilon') \leq \tau_i(\varepsilon) \leq 1 + \exp \{C_2 |\bar{B}(i, \ell_i(\varepsilon''))|\} , \quad (0.8)$$

where $|\bar{B}|$ denotes the number of sites in the ball \bar{B} . In a finite dimensional setting one has $|\bar{B}(\ell)| \sim \ell^d$, but Eq. (0.8) is valid for any topology of the interaction graph. The small thresholds ε' and ε'' are functions of ε which go to zero when ε vanishes, and $C_{1,2}$ are numerical constants which depends on the microscopic details of the Hamiltonian and of the dynamics.

Let us make a series of remarks on this result:

- For simplicity we have explained this relationship between length and time scales for a discrete system of Ising spins, with arbitrary interactions. Its extension to more general discrete degrees of freedom is simple and was the case considered in (10). It is natural to expect that a similar result will hold for particle systems evolving in the continuum, for instance by means of a coarse grained occupation number field, see e.g. (15).
- The relationship between ℓ_i and τ_i holds site by site. This is particularly important for inhomogeneous systems with quenched disorder, where the correlation lengths and times can vary wildly from site to site.
- In the limit of zero temperature the constant C_2 will diverge: the presence of trivial “energetic barriers” can lead to very large correlation times without a growing correlation length.
- The lower and upper bound in Eq. (0.8) are widely separated when ℓ grows, which could suggest that the bounds are very far from optimal. However it can be argued that with the very weak hypotheses made for its derivation, this result can only be marginally enhanced (i.e. at the level of the numerical constants and with a dynamical exponent $z \geq 2$ in the lower bound). Indeed both bounds can be saturated in the low/high temperature regimes of some models which enters in the range of validity of the result (see below for a discussion of diluted mean-field models).

- We would like to emphasize the *static* character of the point-to-set definition of the correlation length. Indeed the expression of the correlation function stated in Eq. (0.3) involves only equilibrium averages, and does not make any reference to the dynamical evolution of the system. Of course if one wants in practice to evaluate this function for a system or a model which does not admit an analytical solution, Monte Carlo simulations will probably have to be used to generate thermalized configurations of the full and constrained systems, yet this dynamics is here only a computational tool and not a part of the definition.
- The dependence of the correlation length and time on the arbitrary threshold ε may look rather unsatisfactory at first sight. Fortunately this is not a real issue for glassy systems: one expects for them a discontinuous behaviour upon approaching the glass transition. The spatial and temporal correlation function decay to zero in a two-step fashion, with the appearance of a growing plateau. As long as ε is smaller than the height of the plateau (called Edwards-Anderson or non-ergodicity parameter) the asymptotic behaviour of $\tau(\varepsilon)$ and $\ell(\varepsilon)$ is essentially independent on the choice of this threshold. This is however a concern for more conventional critical phenomena where the order parameter grows continuously at the transition.
- It should be acknowledged that these bounds do not apply directly for kinetically constrained models (KCM) (16; 17). As a matter of fact the equilibrium measure of these models is a trivial product measure factorized over the sites, hence the correlation length as defined above is always equal to 1. However the dynamical rules defining the KCM violates a technical assumption of permissivity which is necessary for the derivation of these bounds.

0.2.4 Determination of the correlation length in finite dimensional systems

In the following subsection we shall give some explanations on how these bounds can be proven, then the focus of the rest of the chapter will be put on two families of models where analytical computations can be pushed further. Before that we want however to mention some papers, mostly numerical, where finite dimensional models have been investigated with a perspective somehow related to the point-to-set correlation function.

To the best of our knowledge the first papers where glassy systems in confined geometry with boundary conditions self-consistently generated according to the prescription described in the previous sub-sections were in ref. (18). These works investigated the effect of the presence of a wall or confining geometries on the dynamics of Lennard-Jones binary mixtures.

More recent literature has focused on the thought experiment of (9). In (19) a plaquette spin model of a glass was studied analytically and numerically. The effect of boundary conditions on finite size subsystems could be analyzed and led to a determination of a static correlation length along the lines of the thought experiment of (9).

A binary mixture of soft-sphere particles (i.e. a fragile glass-former liquid modeled microscopically with particles in the continuum) was considered in (15; 21; 20). The

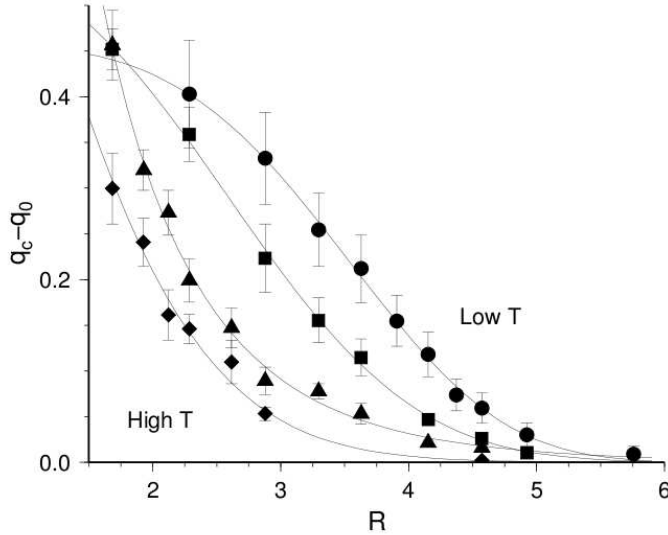


Fig. 0.3 Point-to-set correlation function for a binary mixture of soft-sphere particles, from (21). When the temperature is lowered the influence of the boundary of a spherical cavity persists for larger radius R .

procedure described above of freezing an equilibrium configuration outside a cavity of a given radius and thermalizing its interior was thus implemented with Monte Carlo simulations. This led to a demonstration of the growth of the static correlation length upon lowering the temperature of the liquid. In Fig. 0.3 we reproduce a result of (21), which shows the point-to-set correlation as a function of the radius of the cavity, for various temperatures. The reader is also referred to (15; 21; 20) for the interpretation of these results along the lines of RFOT and for a critical discussion of the scaling exponents of RFOT.

0.2.5 Tools for the proof

Couplings. In this subsection we shall sketch in an informal way the method of proof of Eq. (0.8), the reader being referred to (10) for the details. We want in particular to introduce a very useful probabilistic concept on which the proof of both the upper and the lower bounds of (0.8) relies, namely the construction of a coupling between stochastic processes (22). Let us first explain what is a coupling on the simplest case of two random variables, for instance two biased coins. The first coin $X^{(1)}$ takes value *Head* with probability p_1 , *Tail* otherwise, while the probability of *Head* of the coin $X^{(2)}$ is p_2 . A coupling of these two biased coins is a random variable $(X^{(1)}, X^{(2)})$ which can take four values $\{(H, H), (H, T), (T, H), (T, T)\}$, such that if one observes only the first (resp. second) element of the couple $(X^{(1)}, X^{(2)})$, one sees *Head* occurring with probability p_1 (resp. p_2). Obviously one trivial way to construct such a coupling is to take $X^{(1)}$ and $X^{(2)}$ as independent copies of the original biased coins. The power

of the notion of coupling relies in the possibility to introduce a dependency between the two elements of the couple, without spoiling the partial (marginal) frequency of observations of head in the first or second position. It is indeed easy to realize that there exists an infinity of couplings of these two biased coins parametrized by a real number. Let us give one explicit example. Suppose without loss of generality that $p_1 \geq p_2$, and set the value of the coupling to be

$$(X^{(1)}, X^{(2)}) = \begin{cases} (H, H) & \text{with probability } p_2, \\ (H, T) & \text{with probability } p_1 - p_2, \\ (T, T) & \text{with probability } 1 - p_1. \end{cases} \quad (0.9)$$

One can easily check that this is indeed a coupling (the marginal probabilities for the Head of the two coins are respectively p_1 and p_2), and that, for given values of p_1 and p_2 , it minimizes the probability that $X^{(1)} \neq X^{(2)}$. For this reason it is termed the *greedy coupling* of the two random variables. In particular if the two coins are identical, $p_1 = p_2$, then $X^{(1)}$ is always equal to $X^{(2)}$ in this coupling.

Lower bound. This notion of coupling extends naturally to random variables more complicated than biased coins, and also to stochastic processes, that is sequences of random variables indexed by a time parameter. The proof of the lower bound in Eq. (0.8) relies indeed on such a construction that we shall now explain.

Let us choose a variable i and a positive integer ℓ , and denote as above B (resp. \bar{B}) the outside (resp. inside) of the ball of radius ℓ around i . Consider now the stochastic process $(\underline{\sigma}^{(1)}(t), \underline{\sigma}^{(2)}(t))$, where two configurations of the same system evolves simultaneously, defined by the following rules:

- at the initial time $t = 0$, the two configurations coincide, $\underline{\sigma}^{(1)}(0) = \underline{\sigma}^{(2)}(0) = \underline{\sigma}$, with $\underline{\sigma}$ drawn from the equilibrium Gibbs-Boltzmann measure.
- at any time $t > 0$ where a variable j attempts an update of its value, both configurations are modified together according to:
 - * if $j \in B$, the configuration $\underline{\sigma}^{(2)}(t)$ is kept unchanged, while the spin $\sigma_j^{(1)}(t)$ is flipped or not according to the transition rates $W(\underline{\sigma}^{(1)}(t) \rightarrow \underline{\sigma}')$.
 - * if $j \in \bar{B}$, one determines the probability of $\sigma_j^{(1)}(t)$ (resp. $\sigma_j^{(2)}(t)$) right after the update according to $W(\underline{\sigma}^{(1)}(t) \rightarrow \underline{\sigma}')$ (resp. $W(\underline{\sigma}^{(2)}(t) \rightarrow \underline{\sigma}')$). Then the new values of $(\sigma_j^{(1)}(t), \sigma_j^{(2)}(t))$ are drawn according to the greedy coupling (as defined above) of these two Ising spin random variables.

Observed separately each element of this coupling corresponds :

- for $\underline{\sigma}^{(1)}(t)$ to the original dynamics of the whole system.
- for $\underline{\sigma}^{(2)}(t)$ to the equilibrium dynamics for the inside of the ball \bar{B} , submitted to a time-independent boundary condition in B , with $\underline{\sigma}_B^{(2)}(t)$ fixed forever to the value $\underline{\sigma}_B$ it has at time $t = 0$.

It turns out that the original temporal and point-to-set correlation functions can be computed from appropriate averages over this coupling, that we shall still denote $\langle \dots \rangle$ with a slight abuse of notation. Assuming that the equilibrium magnetization $\langle \sigma_i \rangle$ vanishes to simplify the discussion, one realizes that $C_i(t) = \langle \sigma_i^{(1)}(0) \sigma_i^{(1)}(t) \rangle$, while

$G(i, B)$ is the limit of $\langle \sigma_i^{(2)}(0) \sigma_i^{(2)}(t) \rangle$ as t goes to infinity. To obtain the lower bound of Eq. (0.8) one has to relate in some way the behavior of the spatial and temporal correlation functions. From the above observation this translates into a comparison of the value of σ_i in the two processes $\underline{\sigma}^{(1)}(t)$ and $\underline{\sigma}^{(2)}(t)$. The idea of the proof is then to exploit the properties of the above defined coupling. In fact for “small” times, that is of order smaller than ℓ , most probably $\sigma_i^{(1)}(t) = \sigma_i^{(2)}(t)$. Indeed, at initial times the two configurations coincide everywhere in the system. Moreover, when $j \in \bar{B}$ tries to update, if the two configurations coincide on j and its immediate neighborhood, then necessarily $\sigma_j^{(1)} = \sigma_j^{(2)}$ right after the update, because of the use of the greedy coupling of the two update probabilities. In other words, disagreement between the two configurations can only take birth in the outside B of the ball of radius ℓ , and must propagate from the surface of the ball to its center (23; 24).

Let us rephrase this reasoning with more explicit formulas. We start from a simple inequality on the point-to-set correlation function,

$$G(i, B) = \lim_{t \rightarrow \infty} \langle \sigma_i^{(2)}(0) \sigma_i^{(2)}(t) \rangle \leq \langle \sigma_i^{(2)}(0) \sigma_i^{(2)}(t) \rangle, \quad (0.10)$$

which holds for any value of $t \geq 0$. Indeed the equilibrium auto-correlation functions of reversible Markov processes are decreasing in time¹. To relate the two coupled processes let us define the indicator function $X(t) = \delta_{\sigma_i^{(1)}(t), \sigma_i^{(2)}(t)}$. We can thus upper-bound the spatial correlation function as

$$\begin{aligned} G(i, B) &\leq \langle \sigma_i^{(1)}(0) \sigma_i^{(1)}(t) \rangle - \langle \sigma_i^{(1)}(0) \sigma_i^{(1)}(t) (1 - X(t)) \rangle + \langle \sigma_i^{(2)}(0) \sigma_i^{(2)}(t) (1 - X(t)) \rangle \\ &\leq \langle \sigma_i^{(1)}(0) \sigma_i^{(1)}(t) \rangle + 2 \langle (1 - X(t)) \rangle \\ &= C_i(t) + 2 \mathcal{P}_{\text{dis}}(t), \end{aligned} \quad (0.11)$$

where $\mathcal{P}_{\text{dis}}(t)$ is the probability that the two parts of the coupling disagrees on the value of σ_i at time t . As explained above disagreement between the two configurations of the coupling has to travel from the boundary of B towards i along a sequence of ℓ adjacent spins on a path from B to i . An upper bound on $\mathcal{P}_{\text{dis}}(t)$ can thus be obtained by multiplying the number of such paths with the probability that in the interval of time $[0, t]$ all ℓ sites of a given path attempts to update their configurations in the right order (from the boundary inwards). The first factor is obviously smaller than the maximum connectivity of a spin raised to the power ℓ . Because the times where the spin attempts an update form a Poisson process the second factor is the probability than a Poisson random variable of average t is greater than ℓ , and this last probability is smaller than $(e t / \ell)^\ell$. Putting these two factors together one obtains that $\mathcal{P}_{\text{dis}}(t) \leq (C t / \ell)^\ell$, where C is a constant which depends on the connectivity of the interaction graph. Now if one sets $t = \tau_i(\varepsilon)$, the r.h.s. of (0.11) can be made smaller than 2ε by taking ℓ larger than some constant multiplied by $\tau_i(\varepsilon)$, hence the lower bound in Eq. (0.8).

¹This is a simple property that can be proven using the spectral decomposition of the evolution operator $W(\sigma \rightarrow \sigma')$.

Upper bound. The upper bound of Eq. (0.8) is obtained by showing that the autocorrelation function $C_i(t)$ of the i -th spin is weakly sensitive to the configuration of the system out of the ball of radius $\ell_i(\varepsilon)$. One can thus approximate $C_i(t)$ with the value it would have in the system made only of the interior \bar{B} of the ball of radius $\ell_i(\varepsilon)$. It is natural that the autocorrelation time of the latter cannot grow faster than exponentially in its volume. Consider indeed an arbitrary system with n variables, and the following coupling between two copies of its dynamics. It is initialized with two arbitrary configurations $(\underline{\sigma}^{(1)}(0), \underline{\sigma}^{(2)}(0))$, and one performs at later times the updates of $(\sigma_j^{(1)}(t), \sigma_j^{(2)}(t))$ according to the greedy coupling of the two transition rates. This implies that as soon as the two copies coincide, they remain the same for all subsequent times. Moreover we assume the dynamics to be “permissive”, that is there is a constant $\kappa > 0$ such that when j attempts an update, irrespectively of the neighborhood of j in $(\underline{\sigma}^{(1)}, \underline{\sigma}^{(2)})$, the probability that $\sigma_j^{(1)} = \sigma_j^{(2)}$ after the update is larger than κ . This condition of permissivity is satisfied at any strictly positive temperature if there are no hard constraints in the model (no infinite energy configurations), with possibly κ vanishing when $T \rightarrow 0$. We can upper-bound the relaxation time by the coalescence time of the coupling: if for two arbitrary initial configurations (as different as they can be) the coupled dynamics has coalesced at a given time t_0 , hence “forgotten” its initial conditions, then the equilibrium dynamics of a single configuration would have as well. What remains to be proven is that, with a large probability, this coalescence time is not larger than exponential in the number of variables n . This follows from considering a particular sequence of update events that brings the two evolving copies of the system to coincide, namely that all variables have attempted to update at least once, and that their last update brought the variables to the same value in the two parts of the coupling. The probability of the last condition is by definition larger than κ^n , hence on time intervals larger than κ^{-n} coalescence is very probable.

0.3 Computation of the correlation function in mean-field (random graph) models

In this and the next section we shall discuss simplified models, of mean-field nature (in a sense that shall be precised), for which analytical computations of the point-to-set correlation function are possible.

0.3.1 A reminder on mean-field glassy models

Many researchers agree that important insights on the physics of glassy systems have been gained by the study of apparently remote models, namely mean-field spin glasses with multi-spin interactions. The paradigmatic example is the so-called p -spin model, with $p \geq 3$, defined by the Hamiltonian

$$E(\underline{\sigma}) = - \sum_{1 \leq i_1 < \dots < i_p \leq N} J_{i_1 \dots i_p} \sigma_{i_1} \dots \sigma_{i_p} , \quad (0.12)$$

where the $J_{i_1 \dots i_p}$ are independent Gaussian random variables of zero mean and variance $\mathbb{E}[J_{i_1 \dots i_p}^2] = \frac{p!}{2N^{p-1}}$. In the Ising version of the model the degrees of freedom are $\sigma_i = \pm 1$, while the σ_i are reals in the spherical case, with the additional constraint

$\sum_i \sigma_i^2 = N$. The properties of this model have been extensively studied, we refer the reader to the lecture notes (25; 26; 27) and references therein for the references to the original works. We shall content ourselves here with a very brief reminder of its salient features. From a thermodynamical point of view, the free-energy of this model exhibits a non-analytic behaviour at the critical temperature T_c (also called Kauzmann temperature). However the dynamical properties of the model changes at the dynamic transition temperature $T_d > T_c$: the Gibbs measure gets split onto an exponential number of pure states, the equilibration time of the system diverges in the thermodynamic limit for $T < T_d$, hence the dynamics exhibit aging (with a non-trivial effective temperature) if the system is initialized in a random configuration. The absence of any thermodynamic singularity at T_d is due to a compensation phenomenon between the exponential degeneracy of the pure states (complexity, or configurational entropy) and the internal free-energy of the pure states, such that the total free-energy of the system in the intermediate phase between T_d and T_c coincides with the analytical continuation of the high temperature (liquid) phase. In technical words one has a one step of replica symmetry breaking (1RSB) behaviour with Parisi breaking parameter $m = 1$. On the contrary at T_c the complexity vanishes, and for $T < T_c$ the system enters a true 1RSB phase with $m < 1$.

Of course the main criticism which can be made against the relevance of such a model for the study of structural glasses is its completely different microscopic nature, in particular because of the quenched disorder present in its definition. The two variations of the p -spin model presented in this and in the next section shall not escape this criticism, yet they partially cure some of the pathologies of the model and present an even richer phenomenology, which motivates the theoretical interest for them.

0.3.2 Definition of diluted mean-field models

The model defined by the Hamiltonian (0.12) together with the above stated variance of the couplings constants $J_{i_1 \dots i_p}$ will be termed the fully-connected p -spin model. Indeed all of the $\binom{N}{p}$ possible interactions between p -uplets of spins are present in the system, even if each of them is individually weak in order to have an extensive scaling of the Hamiltonian in the thermodynamic limit. In this case each spin interacts with all the others, in other words the distance $d(i, j)$ between any pair of spins defined in Sec. 0.2.2 is equal to one. This peculiarity, very different from the finite-dimensional models with short-range interactions where any degree of freedom interacts only with a finite number of neighbors, can be cured with the following definition of the coupling constants:

$$J_{i_1 \dots i_p} = \begin{cases} \pm 1 & \text{with probability } \alpha \frac{p!}{2N^p} \\ 0 & \text{with probability } 1 - \alpha \frac{p!}{N^p} \end{cases} . \quad (0.13)$$

This case will be called the diluted p -spin model. At variance with the fully-connected case, only an extensive number (concentrated around its average αN) of interactions are now present, but each of them is strong (of order 1). Moreover a short computation reveals that the degree of one spin, that is the number of interactions it belongs to, converges in the thermodynamic limit to a Poisson random variable of average αp , hence finite with respect to the system size N .

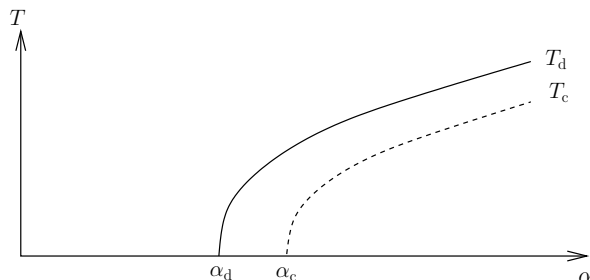


Fig. 0.4 Shape of the phase diagram for the diluted p -spin model.

This kind of diluted model, pioneered in the case $p = 2$ by Viana and Bray (28), can be viewed as intermediary between fully-connected and finite-dimensional ones. They share with the latter the finiteness of the connectivity of each degree of freedom, but are mean-field as the former ones. Indeed there is no a priori underlying Euclidean space in their definition. This allows for detailed analytical computation of their properties, and provides a family of models where the Bethe-Peierls approximation is actually exact in the thermodynamic limit. Moreover there is one more control parameter besides the temperature, namely the “density” parameter α which controls the number of interactions present in the system.

There has been an important research effort in the last decades in the community of statistical mechanics of disordered systems to develop analytical tools for tackling such diluted spin-glasses models. An important motivation has been the intimate connection between these models and random combinatorial optimization problems, as the k -satisfiability and the coloring of random graphs. An extensive account of this line of research can be found in the recent book (29).

Before turning to some explanations on the computations in diluted models, in particular the determination of the point-to-set correlation function, let us plot in Fig. 0.4 the shape of the phase diagram in the (density α , temperature T) plane. The two transition temperatures T_d and T_c of the fully-connected model (which corresponds to the $\alpha \rightarrow \infty$ limit up to a rescaling of the energy) becomes two lines of transitions, which ends up at zero temperature for finite values of the connectivity α , respectively α_d and α_c . The zero-temperature properties of this model have been largely studied in the context of optimization problems (where it is known as XORSAT), the thresholds α_d and α_c corresponding there to the clustering and satisfiability transitions (30; 31).

0.3.3 Computation of the correlation function

We shall now explain the main steps in the computation of the point-to-set correlation function in mean-field diluted systems. Let us first discuss the properties of the (random) factor graph associated with the diluted p -spin model defined by Eqs. (0.12,0.13). To make contact with the general definitions we rewrite it as

$$E(\underline{\sigma}) = \sum_a E_a(\underline{\sigma}_{\partial a}), \quad E_a(\underline{\sigma}_{\partial a}) = -J_a \prod_{i \in \partial a} \sigma_i, \quad (0.14)$$

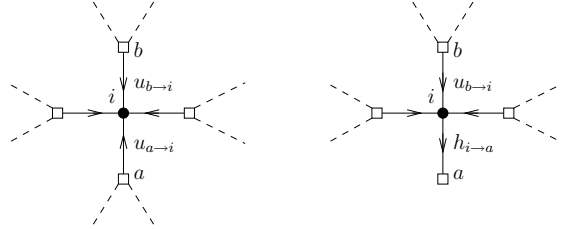


Fig. 0.5 Pictorial representation of the recursive computation on a tree. Left: the effective magnetic field H_i is obtained from the effective fields in the sub-trees $F_{a \rightarrow i}$, see Eq. (0.16). Right: the construction of the field for $F_{i \rightarrow a}$ from the $F_{b \rightarrow i}$, as shown in the second part of Eq. (0.17).

where we have only retained the p -uplets with a non-vanishing coupling constant and renumbered them in terms of the interaction index a . Each interaction a involves p variables, while each variable appears in a random number of interactions, which is easily found to be a Poisson random variable of average αp . What is slightly less obvious is the fact that these random factor graphs have a local tree structure, that is short loops are relatively rare, and only loops of length of order $\log N$ begin to proliferate in the thermodynamic limit ($N \rightarrow \infty$ with α finite). It is this locally tree-like property which allows for analytical computations in these models; note that this property is shared by other definitions of the random factor graph model, in particular with degree distributions other than Poissonian, for instance deterministic.

Let us forget for a moment the existence of (long) loops in the factor graph and see how the problem can be solved easily on a finite tree. The key point is the natural recursive structure of a tree: removing a vertex from a tree leads to a set of smaller sub-trees, which, by definition, are disconnected one from the others. So if one can solve the considered problem on trees of some given size, and glue together the solutions to compute the solution on the concatenated tree, then by recurrence the solution can be found for any tree. Consider for instance the computation of the local magnetization $\langle \sigma_i \rangle$ of a spin in a tree factor graph. According to the recursive strategy just explained, this can be expressed in terms of the magnetization in the sub-trees $F_{a \rightarrow i}$ where only one interaction a around i is retained, in formula one defines the effective magnetic field H_i acting on i ,

$$\langle \sigma_i \rangle = \tanh(\beta H_i) , \quad (0.15)$$

and deduces the latter from the effective fields in the sub-trees $F_{a \rightarrow i}$,

$$H_i = \sum_{a \in \partial i} u_{a \rightarrow i} . \quad (0.16)$$

This relation is represented schematically on the left panel of Fig. 0.5. These in turns can be computed from the effective fields in the sub-trees of the form $F_{j \rightarrow a}$, in which all interactions around the variable j except a is retained,

$$u_{a \rightarrow i} = f_{a \rightarrow i}(\{h_{j \rightarrow a}\}_{j \in \partial a \setminus i}) , \quad h_{i \rightarrow a} = \sum_{b \in \partial i \setminus a} u_{b \rightarrow i} , \quad (0.17)$$

xx *Abstract*

see the right panel of Fig. 0.5 for an illustration. The function $f_{a \rightarrow i}$ depends on the precise form of the interaction energy E_a ; in the case of the p -spin interaction defined in Eq. (0.14) one finds

$$u_{a \rightarrow i} = \frac{1}{\beta} \operatorname{arctanh} \left[\tanh(\beta J_a) \prod_{j \in \partial a \setminus i} \tanh(\beta h_{j \rightarrow a}) \right] ; \quad (0.18)$$

the present discussion applies to any kind of interactions E_a , provided one takes the function $f_{a \rightarrow i}$ corresponding to the model under study.

To summarize, the equilibrium properties of a tree factor graph model can be obtained by solving the recursion equations (0.17) for the effective fields $\{h_{i \rightarrow a}, u_{a \rightarrow i}\}$ living on the directed edges of the factor graph. These equations admit a unique solution which can be easily obtained by starting from the leaves of the tree (the variables with a unique neighboring interaction), where the boundary condition is $h_{i \rightarrow a} = 0$.

We can now proceed with the computations of the conditional averages $\langle \dots \rangle_{\underline{\sigma}_B}$, where the configurations of the variables in a subset B of the variables is fixed to $\underline{\sigma}_B$. A moment of thought reveals that this is a simple modification of the previous computation. In fact one has to look for a set of effective fields $\{h_{i \rightarrow a}^{\underline{\sigma}_B}, u_{a \rightarrow i}^{\underline{\sigma}_B}\}$, which depends on the imposed configuration $\underline{\sigma}_B$. They obey the same recursive equations (0.17), but with an additional boundary condition: $h_{i \rightarrow a}^{\underline{\sigma}_B} = \sigma_i \times \infty$ if $i \in B$. Indeed a fixed variable feels an infinite effective field (positive or negative according to the value it is fixed to). Once the fields $\{h_{i \rightarrow a}^{\underline{\sigma}_B}, u_{a \rightarrow i}^{\underline{\sigma}_B}\}$ have been determined on all edges of the factor graph one obtains in a simple way the conditional magnetizations, for instance

$$\langle \sigma'_i \rangle_{\underline{\sigma}_B} = \tanh(\beta H_i^{\underline{\sigma}_B}) , \quad H_i^{\underline{\sigma}_B} = \sum_{a \in \partial i} u_{a \rightarrow i}^{\underline{\sigma}_B} . \quad (0.19)$$

To complete the computation of the correlation function defined in equation (0.3), one has to average the correlation $\sigma_i \langle \sigma'_i \rangle_{\underline{\sigma}_B}$ with respect to σ_i and $\underline{\sigma}_B$, which are both parts of a reference equilibrium configuration $\underline{\sigma}$. The generation of an equilibrium configuration on a tree factor graph is most naturally done in a recursive, broadcasting like, way. This means that one has first to choose the value of a reference variable, say i , according to its marginal probability law. The latter is known on a tree, since the probability of σ_i to be +1 in an equilibrium configuration is by definition $e^{\beta H_i} / (2 \cosh(\beta H_i)) = (1 + \langle \sigma_i \rangle) / 2$. Once the value of σ_i is fixed in this way, the problem of the generation of the other variables decouples between the various branches emanating from i , thanks again to the tree structure of the factor graph. One can treat independently each interaction a around i , and generate the value of the other variables appearing in a , $\underline{\sigma}_{\partial a \setminus i}$, conditional on the value of σ_i . The correct probability law for this generation reads

$$\mu(\underline{\sigma}_{\partial a \setminus i} | \sigma_i) = \frac{1}{z} \exp \left[-\beta E_a(\sigma_i, \underline{\sigma}_{\partial a \setminus i}) + \beta \sum_{j \in \partial a \setminus i} h_{j \rightarrow a} \sigma_j \right] , \quad (0.20)$$

where z stands for a normalization constant. Once all the variables at distance 1 from i have been fixed, one can proceed in the same way with variables at distance 2, and so on and so forth until the complete configuration $\underline{\sigma}$ has been generated.

We can now wrap together the recursive computation of the conditional magnetizations and the recursive broadcast generation of the reference equilibrium configuration. We shall indeed define $P_{i \rightarrow a}^{\sigma_i}(h'_{i \rightarrow a})$ as the (density of) probability that $h_{i \rightarrow a}^{\underline{\sigma}_B}$ is equal to $h'_{i \rightarrow a}$ when $\underline{\sigma}_B$ is part of an equilibrium configuration $\underline{\sigma}$ drawn conditional on the value of σ_i . A similar definition holds for $Q_{a \rightarrow i}^{\sigma_i}(u'_{a \rightarrow i})$; one can derive recursion relations between these probability distributions,

$$P_{i \rightarrow a}^{\sigma_i}(h'_{i \rightarrow a}) = \int \prod_{b \in \partial i \setminus a} dQ_{b \rightarrow i}^{\sigma_i}(u'_{b \rightarrow i}) \delta \left(h'_{i \rightarrow a} - \sum_{b \in \partial i \setminus a} u'_{b \rightarrow i} \right), \quad (0.21)$$

$$Q_{a \rightarrow i}^{\sigma_i}(u'_{a \rightarrow i}) = \sum_{\underline{\sigma}_{\partial a \setminus i}} \mu(\underline{\sigma}_{\partial a \setminus i} | \sigma_i) \int \prod_{j \in \partial a \setminus i} dP_{j \rightarrow a}^{\sigma_j}(h'_{j \rightarrow a}) \delta(u'_{a \rightarrow i} - f_{a \rightarrow i}(\{h'_{j \rightarrow a}\}_{j \in \partial a \setminus i})), \quad (0.22)$$

complemented with the boundary condition $P_{i \rightarrow a}^{\sigma_i}(h'_{i \rightarrow a}) = \delta(h'_{i \rightarrow a} - \sigma_i \infty)$ when $i \in B$. From the solution of these recursion equations one finally obtains

$$G(i, B) = \sum_{\sigma_i} \sigma_i \frac{e^{\beta \sigma_i H_i}}{2 \cosh(\beta H_i)} \int \prod_{a \in \partial i} dQ_{a \rightarrow i}^{\sigma_i}(u'_{a \rightarrow i}) \tanh \left(\beta \sum_{a \in \partial i} u'_{a \rightarrow i} \right) - \tanh^2(\beta H_i). \quad (0.23)$$

The computation of the point-to-set correlation function we just presented is exact for any model whose factor graph is a finite tree. This is not precisely the case of problems on random graphs, as for instance the diluted p -spin model defined by Eqs. (0.12,0.13). In such models the factor graph is only locally tree-like, loops do exist but most of them have a length which diverge in the thermodynamic limit. In consequence the properties of random graph models can be inferred from such computations on finite trees, provided one takes into account the presence of the loops as self-consistent boundary conditions. This kind of reasoning has been extensively developed in the recent years under the name of the cavity method (32; 29), which is equivalent to the replica method (33) yet more practical for diluted systems. Following this methodology one can perform the average of the point-to-set correlation function (0.23) with respect to the quenched disorder of the model. Without entering the details, this leads to functional recursion equations of the form $P_{\ell+1} = F[P_\ell]$, where P is a probability distribution over real numbers (the h' in (0.21)), and the recursion is over the radius ℓ of the ball on which the correlation is computed. Numerical algorithms to deal with such equations between probability distributions have been extensively used to solve the equations of the cavity method. The idea, known in this context as population dynamics (32), is to approximate a probability distribution by a sample of elements, with an empirical distribution as close as possible to the true distribution.

We show in the left panel of Fig. 0.6 the results of such a computation for the average point-to-set correlation, as a function of the radius of the ball, in the case of the

$p = 3$ diluted model. The density parameter $\alpha = 1$ is larger than the zero-temperature limit $\alpha_d \approx 0.818$ of the dynamic transition line (recall the sketch of Fig. 0.4). Indeed one clearly sees a plateau developing a diverging length upon decreasing the temperature towards $T_d(\alpha) > 0$. As discussed above the presence of this plateau makes the correlation length $\ell(\varepsilon)$ asymptotically independent of the precise choice of ε , as long as it is smaller than the plateau value. This length is plotted in the right panel of Fig. 0.6 as a function of temperature. As the dashed line shows the divergence of the length occurs with a critical exponent $1/2$, i.e. $\ell(\varepsilon) \sim (T - T_d(\alpha))^{-1/2}$. One can expect this exponent to be generic for almost all random graph models with such a discontinuous transition. It is indeed a natural consequence of the recursive structure of the equation underlying the computation, namely $P_{\ell+1} = F[P_\ell]$. In the liquid phase the only fixed point of the equation $P = F[P]$, reached when $\ell \rightarrow \infty$, corresponds to a vanishing correlation. When the parameters (α, T) are taken to the glassy phase a bifurcation in this fixed point equation occurs, a non-trivial solution with a strictly positive correlation appears discontinuously. To simplify the discussion let us consider a toy model where the recursion is upon a real x instead of a function P , $x_{\ell+1} = f(x_\ell)$ (this corresponds actually to the zero temperature limit of the diluted p -spin model, see (34) for more details). The behaviour of the function f upon approaching such a discontinuous bifurcation is shown in Fig. 0.7. It is then a simple exercise to expand the function f when its parameter is slightly in the liquid phase, and its argument x is around the value of the close-by bifurcation, and to show in such a way that the length of the plateau in x_ℓ does indeed diverge with an exponent $1/2$. The functional nature of the recursion in the general computation should not spoil this argument, one can thus expect to find generically such an exponent for the divergence of the point-to-set correlation length in mean-field diluted models.

An important point should be emphasized here : for any kind of transition studied on a Bethe lattice where a correlation length (shortest path on the tree) diverges as $\varepsilon^{-\nu_{\text{tree}}}$ ($\varepsilon \rightarrow 0$ controlling the approach to the critical point), the mean-field exponent of the transition should be deduced as $\nu_{\text{mf}} = \frac{\nu_{\text{tree}}}{2}$ and not ν_{tree} . Indeed the finite connectivity Bethe lattice should be pictured as embedded in an hypercubic lattice of very large dimension d . In this limit a path of length ℓ along the tree corresponds to a random walk (almost independently of the other branches of the tree) on the embedding lattice, with an end-to-end separation of order $\sqrt{\ell}$ in Euclidean distance ². The mean-field value of ν for the transition discussed here is hence $1/4$, we shall come back on this point in Sec. 0.4.1.

0.3.4 Numerical simulations of diluted mean-field models

The mean-field diluted models provide an ideal playground to assess the relevance of the bounds (0.8) between correlation lengths and correlation times: we have seen above how to compute the correlation length in the liquid phase and its divergence at the dynamical transition temperature T_d . In addition the dynamics of these models can be easily investigated with Monte Carlo simulations (for out-of-equilibrium dynamics see for instance (37; 38)). The equilibrium correlation times have been thus determined

²The validity of this argument, which is found for instance in (35; 36), can be checked on the simple example of a particle freely diffusing on a Bethe lattice.

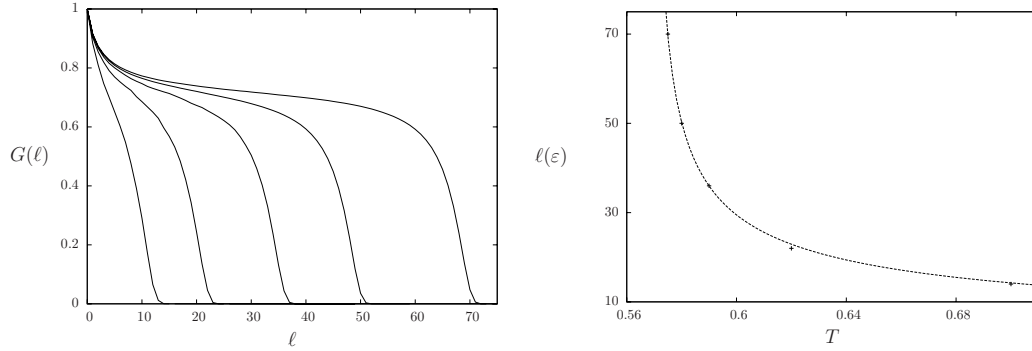


Fig. 0.6 Left: Point-to-set correlation function for the $p = 3$ diluted mean-field model with $\alpha = 1$, from left to right, $T = 0.7, 0.62, 0.59, 0.58$ and 0.575 . Right: the point-to-set correlation length with $\varepsilon = 0.1$, the dashed line is a fit to this data according to the asymptotic expression $\ell_*(\varepsilon) = C(T - T_d(\alpha))^{-1/2}$, with $T_d(\alpha = 1) = 0.51695$.

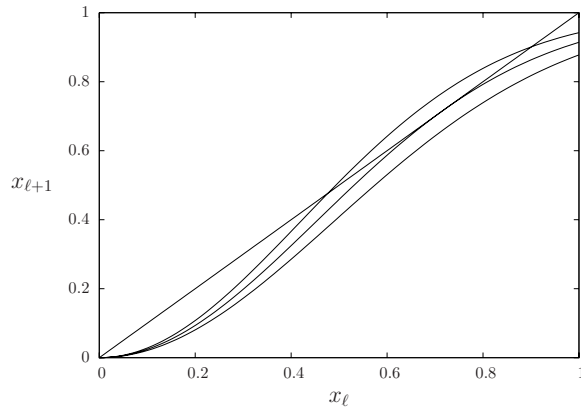


Fig. 0.7 A representation of the bifurcation for the equation $x_{\ell+1} = f(x_\ell)$. From bottom to top the parameters in f are in the liquid phase, precisely at the transition, in the glass phase.

in (10), for a variation of the diluted p -spin model with constant degrees for the spins, and allowed to justify the claim of almost optimality of (0.8) without additional hypotheses. Indeed for $T > T_d$ one finds that the equilibrium correlation time remains finite in the thermodynamic limit, and diverges algebraically when $T \rightarrow T_d^+$. Hence the lower bound of (0.8) could only be improved to include a dynamical exponent z and be promoted to $\tau \geq \ell^z$, with probably $z \geq 2$ for a large class of models. On the contrary in the low temperature phase, $T < T_d$, it is the upper bound of (0.8) which is saturated (up to an improvement of the constant C_2): the equilibrium correlation time diverges exponentially with the size N of the system, and the correlation volume is itself proportional to N .

Coming back to the diluted p -spin model with Poissonian degrees, let us mention a

particular feature which is apparent in the sketch of Fig. 0.4. The dynamic transition line $T_d(\alpha)$ reaches the zero temperature axis at a finite value α_d . The neighborhood of the point $(\alpha = \alpha_d, T = 0)$ thus exhibits a rich crossover phenomenon between low temperature activated dynamics controlled by energy barriers and positive temperature transitions of the schematic Mode Coupling Theory kind (which is an exact description of the $\alpha \rightarrow \infty$ limit (39)). We refer the reader to (34) for more details.

0.3.5 Connection with the replica symmetry breaking formalism

We shall close this section on mean-field diluted systems with a discussion of the relationship between the computation of the point-to-set correlation function and the usual cavity formalism at the level of one step of replica symmetry breaking (1RSB), first unveiled in (40). The existence of such a connection should be expected by the reader accustomed to the fully-connected p -spin model: we argued that in the phase diagram sketched in Fig. 0.4 the transition line $T_d(\alpha)$, defined as the point where the point-to-set correlation length diverges, can be meaningfully called the dynamic transition. Indeed the lower bound in Eq. (0.8) implies a divergence of the equilibrium correlation time on this line. However the large α limit of the diluted p -spin model gives back the fully-connected one. For the latter the dynamic transition has been studied since a long time, and its appearance is known to be related to the static properties of the model studied by various methods, in particular the replica and the TAP ones. One of these characterizations is the existence of a non-trivial solution of the 1RSB equations with the Parisi breaking parameter $m = 1$.

One can indeed recover this equivalent definition of the dynamic transition in generic mean-field diluted systems. Let us come back on the computation on a finite tree presented in Sec. 0.3.3. We introduced there the distribution $P_{i \rightarrow a}^{\sigma_i}(h'_{i \rightarrow a})$ as the probability of $h_{i \rightarrow a}^{\underline{\sigma}_B}$ with respect to the choice of the boundary configuration $\underline{\sigma}_B$ conditioned on σ_i . One can instead define the unconditional version of this distribution, $P_{i \rightarrow a}(h'_{i \rightarrow a})$, which is related to the conditional one by

$$P_{i \rightarrow a}(h'_{i \rightarrow a}) = \sum_{\sigma_i} \frac{e^{\beta h_{i \rightarrow a} \sigma_i}}{2 \cosh(\beta h_{i \rightarrow a})} P_{i \rightarrow a}^{\sigma_i}(h'_{i \rightarrow a}) . \quad (0.24)$$

A similar definition holds for $Q_{a \rightarrow i}(u'_{a \rightarrow i})$. A computation whose details can be found in (40) shows that the conditional equation (0.21) translates into

$$P_{i \rightarrow a}(h'_{i \rightarrow a}) = \frac{1}{\mathcal{Z}_{i \rightarrow a}} \int \prod_{b \in \partial i \setminus a} dQ_{b \rightarrow i}(u'_{b \rightarrow i}) \delta \left(h'_{i \rightarrow a} - \sum_{b \in \partial i \setminus a} u'_{b \rightarrow i} \right) \times \left(\frac{\cosh(\beta h'_{i \rightarrow a})}{\prod_{b \in \partial i \setminus a} \cosh(\beta u'_{b \rightarrow i})} \right) . \quad (0.25)$$

This is nothing but the usual 1RSB equation with $m = 1$ (32) (in general the last term in parenthesis, called reweighting factor or free-energy shift, is raised to the power m). A similar observation holds for the equation on $Q_{a \rightarrow i}$ obtained from (0.23). The 1RSB

equations are usually solved on a random factor graph without any explicit boundary B . In consequence the existence of a non-trivial solution of the usual 1RSB equations with $m = 1$ is equivalent to the presence of long-range point-to-set correlations (with a fictitious boundary sent to infinity).

This computation provides also an alternative interpretation of the 1RSB equations for mean-field diluted systems. $P_{i \rightarrow a}$ is usually considered as the distribution of an effective field with respect to the choice of a *pure state* of the system. This can be intuitively defined for a random graph of large but finite size as a portion of the configuration space sufficiently disconnected from the other pure states, yet a clear-cut mathematical definition is not easy to handle. One can alternatively interpret $P_{i \rightarrow a}$ as a distribution over the boundary conditions of a tree of very large depth. This is precisely the computation done for the point-to-set correlation, i.e. the 1RSB equations with $m = 1$, where the boundary condition is drawn itself from the Gibbs-Boltzmann distribution. One can moreover generalize this interpretation to arbitrary values of m , biasing accordingly the probability distribution of the boundary conditions (41).

0.4 Kac models

A different class of systems in which the computation of PS correlation is possible is provided by Kac models. Kac models are classical tools of statistical physics to study the relationship between finite dimensional systems and their Mean Field counterparts (42; 43; 44). In these models one considers variables interacting through a potential of growing range r_0 and intensity decreasing in such a way as to keep finite the total interaction strength of one particle with the surrounding environment. For any finite values of r_0 the general properties of finite dimensional system such as convexity of free-energy and absence of infinite life metastable states hold. There properties break down in mean-field theory, which holds exactly in the limit of weak long range forces in which r_0 scales as the linear system size L and both lengths tend to infinity together. The relation between the two regimes can be understood studying the so-called Kac limit (42), where one considers a large interaction range $r_0 \rightarrow \infty$ but only after having taken the thermodynamic limit $L \rightarrow \infty$. Remarkably one finds that while the mean-field predictions hold in single phase regions, some of the typical pathologies of mean-field theory, such as the non convex free-energies are removed and the Maxwell construction emerges naturally. The resulting theory is an improved mean field theory that incorporate the spatial dimension, with the possibility of describing inhomogeneous configurations and interfaces. For some systems (see, for instance, Refs. (45; 46)) it has been possible to devise asymptotic expansions around $r_0 = \infty$ which have led to the analysis of decay of metastable states or proofs of the existence of phase transitions. It is natural in the context of glassy systems to address the study of correlation lengths in the Kac limit. This provides a solvable limit case to confront with phenomenological theories based on mean-field ideas(1; 9) and gives rise to a detailed picture with two relevant length scales.

0.4.1 Definition

Disordered models with Kac interactions were first described in (47), the case of spin glass models with pair interactions. Following the general philosophy of this chapter,

here we are interested in more general models with p -body interactions providing a minimal finite dimension modification of the fully connected p -spin model (0.12).

We consider then spins σ_i in the d dimensional hypercube $i \in \Lambda = \{1, \dots, L\}^d$ with periodic boundary condition. The variables σ_i can be of various nature, for example they can be Ising variables $\sigma_i = \pm 1$ or real variables subject to some local spherical constraint as we will specify below. The Kac p -spin Hamiltonian is defined by (48)

$$E(\underline{\sigma}) = - \sum_{i_1, i_2, \dots, i_p \in \Lambda} J_{i_1, \dots, i_p} \sigma_{i_1} \dots \sigma_{i_p} \quad (0.26)$$

where, as for the mean-field model, the coupling constants J_{i_1, \dots, i_p} are independent centered Gaussian variables, but now differently from the mean field model, the variance depends on the mutual distances between the indexes according to:

$$\mathbb{E}[J_{i_1, \dots, i_p}^2] = \frac{1}{r_0^{pd}} \sum_{k \in \Lambda} \psi \left(\frac{|k - i_1|}{r_0} \right) \dots \psi \left(\frac{|k - i_p|}{r_0} \right). \quad (0.27)$$

The function $\psi(x)$ can be chosen somehow arbitrarily, provided it fulfills the following constraints:

- it is positive, $\psi(x) \geq 0$.
- it becomes negligible when its argument is much larger than 1.
- it is normalized such that $\int d^d x \psi(x) = 1$.

These conditions guarantee that only spins within distances of order r_0 have an effective direct interaction. The function ψ can also be used to define a locally spherical model that without changing the physics from the Ising case, allows important simplifications in analytic studies. This is done considering $\sigma_i \in \mathbb{R}$ subject to the conditions $\frac{1}{r_0^d} \sum_{j \in \Lambda} \psi \left(\frac{|i-j|}{r_0} \right) \sigma_j^2 = 1$ in all points of space i . Note that the disorder distribution implies that the Hamiltonian itself has a Gaussian distribution with covariance specified by

$$\mathbb{E}[E(\underline{\sigma}^{(1)})E(\underline{\sigma}^{(2)})] = \sum_i Q_i(\underline{\sigma}^{(1)}, \underline{\sigma}^{(2)})^p, \quad (0.28)$$

where $Q_i(\underline{\sigma}^{(1)}, \underline{\sigma}^{(2)}) = \frac{1}{r_0^d} \sum_j \psi \left(\frac{|i-j|}{r_0} \right) \sigma_j^{(1)} \sigma_j^{(2)}$ measures the similarity of the two configurations $\underline{\sigma}^{(1)}$ and $\underline{\sigma}^{(2)}$ on a ball of scale r_0 around i . Models that compound different values of p can be defined considering gaussian Hamiltonian with correlations $\mathbb{E}[E(\underline{\sigma}^{(1)})E(\underline{\sigma}^{(2)})] = \sum_i \phi(Q_i(\underline{\sigma}^{(1)}, \underline{\sigma}^{(2)}))$. The function $\phi(q)$ should satisfy suitable conditions to define a non-negative covariance matrix.

Following the original suggestion by Kac (42), the scaling of the interaction with r_0 is chosen in such a way to insure the existence of the limit of the free-energy for $r_0 \rightarrow \infty$. Different ways of taking this limit allows to study the relation between systems with finite range interactions and their mean field counterpart. If r_0 is chosen to scale with the system size $r_0 = L \gg 1$ we have back the mean-field limit. All groups of p spins interact and the lattice structure and the space dimension become completely inessential. But one can consider a different procedure, called Kac limit,

where $r_0 \rightarrow \infty$ only after the thermodynamic limit $L \rightarrow \infty$. A requirement for Mean Field to have a qualitative relevance in the description of finite range systems is a smooth r_0 cross-over from $r_0 \ll L$ to $r_0 \sim L$ ($L \gg 1$). Rigorous results connecting the Kac limit to the mean-field limit have been proved in (50; 48), under the technical hypothesis of parity of the function ϕ , $\phi(q) = \phi(-q)$. These findings can be informally and qualitatively stated as follows:

- The free-energy of the Kac model tends for all temperature to the free-energy of the corresponding mean-field model in the Kac limit.
- In the same limit, the structure of the correlation functions on length scales of order of r_0 approaches the structure of mean-field correlations.

The first point is a continuity property, it tells that the mean field limit is a good starting point in the evaluation of the free-energy for large r_0 . Of course this does not necessarily imply that the phase transitions found in mean field are also present for some finite r_0 . For example, it is clear that in 1D the free-energy is an analytic function of temperature for all finite r_0 , despite the fact that the large r_0 limiting function exhibit a phase transition.

The second point clarifies that mean-field approximation is at least capable to capture the local properties of the system. This is particularly interesting at low temperature where it implies that the system behaves as an ideal glass at least locally on length scales of order r_0 . The possibility that this description extends to scales much larger than r_0 in some finite space dimension remains an open question. To go beyond these general rigorous results and study quantitatively the behavior of correlation lengths, tools of theoretical physics and non-rigorous techniques are needed as it will be explained in the next sections.

0.4.2 Effective potential: a Landau free-energy functional for glasses

In this section we would like to review the basic tool of the *glassy effective potential* (52), which has been instrumental in the computation of point-to-set correlation lengths in the Kac model (58).

The effective potential is a Landau kind of free-energy as function of an order parameter explicitly devised to be sensitive to stable or metastable glassy states. While this construction is in principle very general, for sake of simplicity we first expose it in the case of fully connected models, and later explain how to extend the analysis to Kac models. The basic idea is that metastable states can be studied through restrictions of the Boltzmann-Gibbs measure to the surroundings of a representative configuration. One then observes that in glassy systems where equilibrium is composed by an extensive number of metastable states, any equilibrium configuration can be taken as a representative configuration. Let us then choose a random configuration $\underline{\sigma}^0$ according to the equilibrium measure, and consider a second system $\underline{\sigma}$ which is in a constrained equilibrium where the overlap with the reference configuration $q(\underline{\sigma}^{(0)}, \underline{\sigma}) = \frac{1}{N} \sum_i \sigma_i \sigma_i^0$ is fixed to some preassigned values p .³

³Note that we used already the letter p to define the p -spin Hamiltonian. It will be clear from the context to which quantity the notation refers.

The free-energy of this second system, for fixed $\underline{\sigma}^{(0)}$ is

$$F[p, \underline{\sigma}^{(0)}] = -\frac{T}{N} \log Z[p, \underline{\sigma}^{(0)}] \quad (0.29)$$

$$Z[p, \underline{\sigma}^{(0)}] = \sum_{\underline{\sigma}} e^{-\beta E(\underline{\sigma})} \prod \delta(q(\underline{\sigma}^{(0)}, \underline{\sigma}) - p). \quad (0.30)$$

In the thermodynamic limit this is self-averaging with respect to the quenched disorder in the interactions and the choice of the equilibrium configuration $\underline{\sigma}^0$,

$$F[p] = \mathbb{E} \langle F[p, \underline{\sigma}^{(0)}] \rangle, \quad (0.31)$$

where by $\langle \cdot \rangle$ we denoted the average with respect to the equilibrium distribution for $\underline{\sigma}^{(0)}$ and by \mathbb{E} the average with respect to the quenched disorder. The function $F[p]$ can be used as a Landau free-energy as a function of the order parameter to detect and study glassy states. It is customary to define the effective potential $V[p]$ subtracting the unconstrained value of the free-energy, $V[p] = F[p] - F$. This is the large deviation function allowing to evaluate the probability $\mathbb{P}[p]$ of the overlap with a reference configuration

$$\mathbb{P}[p] = \exp(-\beta V[p]) . \quad (0.32)$$

The analysis of the effective potential, which requires the computation of the double average in (0.31) can be performed in mean-field theory through the replica method, or alternatively the cavity method. For the family of models we are interested in, the most general ansatz needed to describe $V[p]$ is of a 1RSB form, that accounts for the possibility of having multiple metastable states. In fully connected models this takes a simpler form with respect to the diluted models described in section 0.3.5. This is just parametrized by the Parisi breaking parameter m and two real variables q_1 and q_0 , which represent respectively the typical value of the overlap between configuration in the same metastable state and in different ones (2). The parameter m can be tuned to select different families of metastable states with different free-energies. If the equilibrium phase is composed by an extensive number of metastable state, corresponding to a non-zero configurational entropy m takes the value $m = 1$.

In the spherical p-spin model, defined by the Hamiltonian (0.12), the effective potential can be computed in a closed form as a saddle point over q_1, q_0 :

$$V[p] = \max_{q_1, q_0} \mathcal{V}(p, q_1, q_0, m) \quad (0.33)$$

$$\begin{aligned} \mathcal{V}(p, q_1, q_0, m) = & -\frac{1}{2}\beta[2\phi(p) - m\phi(q_0) - (1-m)\phi(q_1)] + \\ & \frac{1}{2\beta} \left(\frac{p^2 - q_0}{1 - (1-m)q_1 - mq_0} + \frac{1-m}{m} \log[1 - q_1] - \frac{1}{m} \log[1 - (1-m)q_1 - mq_0] \right) \end{aligned}$$

where we denoted $\phi(q) = \frac{1}{2}q^p$. The shape of the function $V[p]$, which depends on temperature, is sensitive to the existence of metastable states. Indeed, as can be seen in Fig. 0.8, one can identify three model dependent temperatures of interest where

qualitative changes take place. Two of them are the mean-field dynamical transition temperature T_d and the static transition temperature T_c . In addition there is a third temperature T^* , with $T^* > T_d > T_c$, first identified in (52). Above T^* the function V is a convex function with a single minimum at $p = 0$. At T^* an inflection point appears, and below that temperature the potential is non-convex. For temperature between T_d and T^* , the function continues to have a single minimum for $p = 0$. At T_d a local minimum at a value $p = q_{EA} > 0$ develops. In the interval $[T_c, T_d]$, the point $p = 0$ is still the absolute minimum of V . The two minima structure below T_d reflects the partition of the equilibrium measure in disjoint metastable states. The value q_{EA} is the typical overlap between configurations belonging to the same metastable state. For $p = q_{EA}$ $\underline{\sigma}$ is in the state specified by $\underline{\sigma}^{(0)}$. Different metastable states have zero mutual overlap. For $p = 0$ all but the metastable state specified by $\underline{\sigma}^{(0)}$ contribute to the free-energy and $V(0) = 0$. Correspondingly, the difference in free-energy between the two minima equals the system's configurational entropy $\Sigma_\infty(T)$ multiplied by temperature. The configurational entropy vanishes linearly on approaching T_c , $\Sigma_\infty(T) \sim T - T_c$ and the two minima become degenerate. Below that temperature the mean field model is in an ideal glassy state and the two minima remain degenerate.

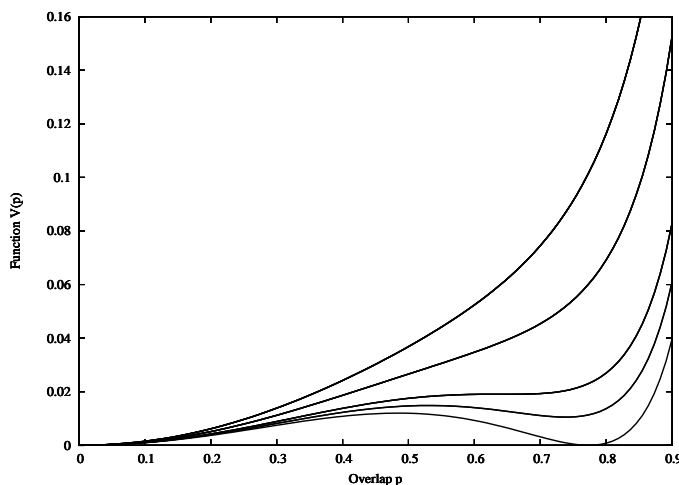


Fig. 0.8 The function $V(p)$ at different temperatures. For comparison with the case of Kac model we consider a Hamiltonian with two body and 4 body interactions with $\phi(p) = 1/2(0.1 \times p^2 + p^4)$. From top to bottom $T = 0.703486 > T^*$, $T = T^* = 0.633137$, $T = T_d = 0.57525$, $T = 0.558049$, $T = T_c = 0.541847$. The function is convex for $T > T^*$. It has an inflection point with positive slope for $T_d < T < T^*$. In the interval $T_c < T < T_d$, $V(q)$ has a local minimum for a temperature dependent value $p = q_{EA}$. The difference $V(q_{EA}) - V(0)$ is (T times) the bulk configurational entropy $V(q_{EA}) - V(0) = T\Sigma_\infty(T)$.

We now generalize the previous construction to Kac models. As before, we use the overlap with an equilibrium reference configuration $\underline{\sigma}^{(0)}$ as an order parameter. In this case however, we are interested in considering the free-energy as a functional

of an order parameter profile that is space dependent. In view of considering large values of the interaction range r_0 it is natural to coarse-grain the order parameter on scales δ such that $\delta \simeq dx r_0 \gg 1$ with $dx \ll 1$ (59; 60). This allows to rescale all lengths $x = i/r_0$ which are then measured in units of the interaction range r_0 . Let us denote $q_x(\underline{\sigma}^{(0)}, \underline{\sigma}) = \frac{1}{\delta^d} \sum_{i \in B_x} \sigma_i^{(0)} \sigma_i$ the local overlap in a square cell B_x of linear size δ labeled by x between two configurations $\underline{\sigma}^{(0)}$ and $\underline{\sigma}$. In complete analogy with the long-range case, one can define an effective potential functional $W[p(x)] = F[p(x)] - F$ as the average free-energy excess for imposing an overlap profile $p(x)$.

$$F[p(x)] = -\frac{T}{N} \mathbb{E} \log Z[p(x), \underline{\sigma}^{(0)}] \quad (0.34)$$

$$Z[p(x), \underline{\sigma}^{(0)}] = \sum_{\underline{\sigma}} e^{-\beta E(\underline{\sigma})} \prod_x \delta(q_x(\underline{\sigma}^{(0)}, \underline{\sigma}) - p(x)). \quad (0.35)$$

We can now relate the point-to-set correlation function to the effective potential. Consider the correlation function between point 0 and the set B considering profiles such that $p(x) = 1$ is fixed for $x \in B$. Observing that the probability of a profile can be written as $\mathbb{P}[p(x)] = \exp(-W(p(x)))$ we find

$$\langle \langle p(0) \rangle_{\underline{\sigma}_B^{(0)}} \rangle = \frac{\int_{\{p(x)=1; x \in B\}} \mathcal{D}p(x) e^{-\beta W[p(x)]} p(0)}{\int_{\{p(x)=1; x \in B\}} \mathcal{D}p(x) e^{-\beta W[p(x)]}}. \quad (0.36)$$

For general values of r_0 the evaluation of the large deviation functional $W[p(x)]$ is a formidable task. Fortunately, in the Kac limit $r_0 \rightarrow \infty$ the computation becomes simpler, it can be stated as a variational problem that generalize to spatially varying functions the saddle point evaluation of (0.34). The region of temperatures $T > T_c$ can be analyzed through the 1RSB theory that we have discussed in several contexts in this chapter. This generalizes the description of the fully-connected case in the fact that the overlap variational parameters become position dependent functions $q_1(x)$ and $q_0(x)$ (the parameter m remains space independent). We give the explicit expression of the effective potential for the p-spin model (0.26) with local spherical constraint, where the dependence on the various parameters can be written in a closed form

$$W[p(x)] = \max_{q_1(x), q_0(x)} r_0^d \int d^d x \left(-\frac{1}{2} \beta \{ 2[\phi(p^*(x)) - \phi(p(x))] - m[\phi(q_0^*(x)) - \phi(q_0(x))] \right. \\ \left. - (1-m)[\phi(q_1^*(x)) - \phi(q_1(x))] \} + \mathcal{V}(p(x), q_1(x), q_0(x), m) \right), \quad (0.37)$$

We have introduced the notation $f^*(x) = \int d^d y \psi(|x-y|) f(y)$ for the convolution with ψ and the function $\mathcal{V}(p, q_1, q_0, m)$ is given by the mean field expression (0.34). Mutating the terminology from mechanics we will call action the argument of the max in (0.37). We notice that for profiles that are inhomogeneous on limited spatial extension W is proportional to the interaction volume r_0^d . The expression (0.37) can be simplified using a (physically harmless) lowest order gradient expansion for the convolution $\phi(f^*(x)) = \phi(f(x)) + c \phi'(f(x)) \nabla^2 f(x)$ with $c = \frac{1}{2d} \int d^d z \psi(|z|) z^2$. This approximation does not affect the physics of the problem while the action takes the familiar field-theoretical form of the integral of a Lagrangian density, dependent on

the various overlap parameters and their spatial derivatives. Notice however that for the expansion to be well behaved one needs $\phi''(q) > 0$ for all q . This is not verified for pure p -spin interactions if $p \geq 3$ which has $\phi''(0) = 0$. For this reason the numerical computations based on this truncation have used functions ϕ of the kind $\phi(q) = \frac{1}{2}(q^4 + aq^2)$, which correspond to a mixed p -spin model with two body and four body interactions. For small enough values of a the model has the same phenomenology as the pure p -spin. Figures are presented for the value $a = 0.1$.

Thanks to the proportionality of the action to the interaction volume r_0^d , the functional integral in the expression (0.36) of the PS correlations can be evaluated by saddle points. We will be then interested in profiles $p(x)$ that are stationary points of the action $\frac{\delta W}{\delta p(x)} = 0$ for $x \in \bar{B}$ with boundary condition $p(x) = 1$ for $x \in B$. These include the absolute minima, that represent equilibrium profiles and directly determine the PS correlation function, but also relative minima, saddle points and maxima that we will associate to metastable states and barriers.

The condition of equilibrium (0.6) discussed in section 0.2.2 has interesting implications on the mutual relation between the overlap functions $q_1(x)$, $q_0(x)$ and $p(x)$. Consider the local overlap $q_x(\underline{\sigma}', \underline{\sigma}'')$, between two replicas with the same constraint $\underline{\sigma}^{(0)}$ on B , and its k -th moment $\mathbb{E}\langle q_x(\underline{\sigma}', \underline{\sigma}'')^k \rangle$. it is possible to show (2) that within the 1RSB formalism

$$\lim_{r_0 \rightarrow \infty} \mathbb{E}\langle q_x(\underline{\sigma}', \underline{\sigma}'')^k \rangle = (1 - m)q_1^k(x) + mq_0^k(x) \quad (0.38)$$

where $q_1(x)$ and $q_0(x)$ are the solution of the maximization problem (0.37). On the other hand, according to (0.6), this expectation value should be simply equal to $\lim_{r_0 \rightarrow \infty} \mathbb{E}\langle q_x(\underline{\sigma}^{(0)}, \underline{\sigma}')^k \rangle = p(x)^k$, thus leading for all k and x to the identity $(1 - m)q_1^k(x) + mq_0^k(x) = p(x)^k$. Two different ways of satisfying this identities are of physical relevance: 1) a simple solution describing equilibrium in a single metastable state, such that for all x

$$q_1(x) = q_0(x) = p(x) . \quad (0.39)$$

2) A solution with $m \rightarrow 1$, for which

$$\begin{aligned} q_0(x) &= p(x) , \\ q_1(x) &> p(x) . \end{aligned} \quad (0.40)$$

This solution (see below) is relevant when ergodicity is broken and the constrained equilibrium is composed by multiple metastable states with a non-zero configurational entropy Σ . According to general principles (62) the configurational entropy can be computed from a solution with the form (0.40) as $\Sigma = -\beta \frac{1}{m^2} \frac{\partial W}{\partial m} |_{m=1}$.

Non-equilibrium stationary profiles $p(x)$, associated to transition states and barriers, will be relevant in our analysis. For these non-equilibrium solutions, there are no restrictions of principle on the functions $q_1(x)$ and $q_0(x)$. Of course the condition $q_0(x) = q_1(x) = p(x)$ can still be used as an approximation. Despite the fact that in some regions this gives rise to clear physical inconsistencies we believe that it predicts the correct scaling of the free-energy of metastable and barrier states with temperature and interaction range. More complex solutions, studied in (69) confirm this point.

Let us stick to the forms (0.39) and (0.40). In both mentioned cases, one gets great simplifications in the variational problem one needs to solve. For example for the ergodic equilibrium profiles (0.39) the effective potential, using the mentioned gradient expansion for the convolution reads:

$$\begin{aligned}
 W[p(x)] &= r_0^d \int d^d x \left(-\frac{c\beta}{2} (\phi'(p(x)) \nabla^2 p(x) + V(p(x))) \right) \\
 V(p) &= -\frac{\beta}{2} \phi(p) - \frac{T}{2} [p(x) + \log(1 - p(x))] .
 \end{aligned}
 \tag{0.41}$$

In the 1RSB solution (0.40) an additional q_1 dependent term proportional to $1 - m$ appears that allow to compute the configurational entropy. It is natural to look for solutions respecting the symmetries imposed by the set B . We will discuss mainly the spherical geometry, where the set B is just the exterior of a spherical cavity, $B = \{x : |x| > \ell\}$ and solutions should only depend on $|x|$. Another interesting choice is the one of planar geometry, where $B = \{x : |x_1| > \ell\}$, with x_1 the first component of the d dimensional vector x , solutions should only depend on x_1 . In both cases it is interesting to study the behavior of the solutions as a function of the cavity size ℓ , that, remember, we measure in units of r_0 as all the lengths. Physical saddle points should be such that in both cases the profile is flat in the center of the cavity $\nabla p(0) = 0$. In both geometries the minimum equations for W can be easily numerically integrated, yielding solutions qualitatively independent from the physical dimension in the spherical case, and strictly independent of the physical dimension in the planar case. The main qualitative features can be obtained in the planar case where the overlap profile can be obtained by quadrature. In fact this case is formally identical to the problem of a 1D Newtonian particle with coordinate p evolving in time in a potential equal to $-V(p)$. Unless otherwise stated the results we will discuss, and in particular the behavior of the different lengths that will be identified, are independent of the geometry and the dimension. We will denote $p(x; \ell)$ the solution $p(x)$ of the variational problem for the boundary conditions fixed at distance ℓ .

0.4.3 The physical picture

The nature of the solutions of the stationary point of (0.41) and the behavior of the PS correlations as a function of the cavity size ℓ reflect the shape of the mean-field potential $V(p)$ that we have discussed in the previous section.

In the “very high” temperature region $T > T^*$ for each value of ℓ , both in the spherical and planar geometries, there is a unique solution of the field equations with the imposed boundary conditions. As a function of ℓ the PS function $p(0; \ell)$ decreases continually from 1 to 0.

At $T = T^*$ an instability develops. Below that temperature one finds a temperature dependent interval of lengths $I = [\ell_0, \ell_d]$ where the field equations admit three distinct solutions. For temperatures in the interval (T_d, T^*) both lengths are finite, while $\ell_d = \infty$ for $T < T_d$. The behavior of $p(0; \ell)$ for different temperatures is depicted in the figure 0.9. The figure also shows the complete profile $p(x; \ell)$ as a function of x for specific values of ℓ and the temperature in the three solutions. According to the value of $p(0; \ell)$, we call the three profiles Low Overlap Solution (LOS), Medium Overlap

Solution (MOS) and High Overlap Solution (HOS). These have different free-energies. The HOS and the LOS one correspond to free-energy absolute or relative minima, the MOS one is a maximum with respect to $p(0; \ell)$.

The structure of the solutions allows to identify three relevant lengths which grow for decreasing temperatures: two metastability lengths ℓ_0 and ℓ_d defining the interval in which three solutions exist, and a thermodynamic length ℓ_c , with $\ell_0 < \ell_c < \ell_d$, for which the HOS and the LOS have the same free-energy. The presence of two free-energy minima separated by a barrier naturally interpreted a metastability phenomenon. The typical relaxation time depends on size of the cavity ℓ and diverges exponentially for $r_0 \rightarrow \infty$ if $\ell_0 < \ell < \ell_d$.

We divide the remaining of this section in the discussion of the equilibrium solutions, the metastable solutions and the unstable solutions for $T < T^*$.

Equilibrium and metastable solutions. Let us consider the behavior of the system in spherical geometry as a function of the ball radius ℓ . Below the length ℓ_0 the HOS is the only minimizer of the free-energy functional, there are no metastable states poorly correlated with the boundary conditions. This absence has consequences in dynamics: any configuration in B chosen as initial condition for the dynamics, evolves in an r_0 independent time to the HOS. Above this length, in the interval $\ell \in (\ell_0, \ell_c)$ the LOS makes its appearance as a free-energy local minimum. Though the HOS is still thermodynamically dominant, metastable states exist such that if they are chosen as initial conditions in relaxation dynamics, they will take a time exponentially large in the interaction volume r_0^d to relax to equilibrium.

The difference in free-energy between the HOS and the LOS decreases upon increasing ℓ , until, for $\ell = \ell_c$ the two free-energy minima are degenerate. As we will discuss later, the length ℓ_c is growing for decreasing temperatures, and diverges for $T \rightarrow T_c$. Above this length the LOS becomes the dominating thermodynamic state. There is a phase transition in ℓ separating a phase strongly correlated with the boundary below ℓ_c , from an essentially uncorrelated phase above. The PS correlation function which should be identified with the value of $p(0; \ell)$ in the thermodynamically dominant solution exhibits a first order jump in $\ell = \ell_c$. Below ℓ_c the system is thermodynamically in an ideal glassy amorphous state where, despite no sign of intrinsic order, the boundary conditions determine the bulk configuration. Conversely, above ℓ_c , the system is in a liquid situation where the boundary has little influence on the bulk. The presence of the transition is reminiscent of the analysis of PS function by Biroli and Bouchaud (9), with ℓ_c thus identified with the mosaic length of phenomenological RFOT (1). This theory postulates a competition between interfacial energy and configurational entropy, the contributions compensating exactly at the transition. However, as we have discussed for generic observables in sec. 0.2.2 (see formula (0.4)), the average energy density for the constrained system is equal in all points of space to its unconstrained equilibrium value. This implies in particular that at the coexistence point both phases should have the same energy density, and therefore entropy, in each point of space. The transition should therefore depend on a different mechanism. Further analysis of the HOS and the LOS presented below reveals that it has the character of a configurational entropy crisis similar to the one that happens at T_c for the infinite system.

In the region $\ell \in (\ell_c, \ell_d)$, the HOS appears to be a local minimum of the free-energy functional. The length ℓ_d marks the limit of metastability of the HOS and was called dynamical length in (58). For $r_0 \rightarrow \infty$ and $\ell \in (\ell_c, \ell_d)$, a system prepared in the configuration $\underline{\sigma}^{(0)}$ at an initial time $t = 0$ would not be able to dynamically relax towards the thermodynamic equilibrium profile. For large but finite r_0 the relaxation time (for the dynamics in a ball of radius ℓ) to the LOS profile can be expected to behave exponentially, $\tau(r_0, \ell, T) \sim \exp(r_0^d \mathcal{B}(\ell, T))$. In other words, for $r_0 \rightarrow \infty$, while the relaxation time is divergent, the barrier (counted in units of the interaction volume) $\lim_{r_0 \rightarrow \infty} \frac{1}{r_0^d} \log \tau(r_0, \ell, T) = \mathcal{B}(\ell, T)$ remains strictly positive. Conversely, for ℓ larger than ℓ_d the relaxation time would remain finite for $r_0 \rightarrow \infty$. ℓ_d appears as the minimal length for which relaxation is possible without barrier jumping. As Fig. 0.10 shows, the dynamic length increases monotonically and diverges as T decreases from T^* on approaching T_d . Generically in the class of models we are interested in, it behaves as

$$\ell_d \sim (T - T_d)^{-\frac{1}{4}}, \quad (0.42)$$

at least below dimension 6. Interestingly, this scaling, first found in (1), coincides with the one obtained for the length ℓ_4 quantifying the typical extension of collective motion in MCT (7; 8) relaxation processes. This seems natural since, in the $r_0 \rightarrow \infty$ limit a set of ideal inhomogeneous MCT equations can be shown to describe the dynamics of the Kac model (63). A simple scaling argument accounts for the above behavior in the present context. For temperatures close to T_d and dimension smaller than $d_c = 6$, the properties of the solutions only depend on V in the vicinity of the inflection point (64). The potential can then be expanded to the cubic order around p_d , its inflection point at T_d , as $V(p, T) = V(p_d, T) + \epsilon a(p - p_d) + b(p - p_d)^3$, where generically the coefficient of the linear term is $\epsilon = T - T_d$ while a and b are positive model-dependent parameters with a weaker temperature dependence. Writing $p - p_d = \varphi$ this gives rise to a cubic field theory

$$W[\varphi] = r_0^d \int d^d x \left(\frac{\epsilon}{2} (\nabla \varphi^2(x)) + a\epsilon \varphi + b\varphi^3 \right), \quad (0.43)$$

whose critical properties dominate the behavior of observable quantities for $\epsilon \rightarrow 0$. In particular, equating the order of magnitude of the different terms in the Lagrangian $\epsilon \varphi \sim \varphi^3 \sim (\nabla \varphi)^2$ immediately leads to a length $\ell_d \sim \epsilon^{-1/4}$. It has been noticed in the context of spinodal theories that the expansion (0.43) cannot be used above dimension 6, and the critical point has a non-universal character (64).

The nature of the LOS is clarified considering the 1RSB solution for $m = 1$ (0.40) we mentioned in the previous section. In the region $\ell > \ell_d$ the LOS is the unique free-energy minimizer and it represents an ergodic state. Conversely, for $\ell_c < \ell < \ell_d$ this solution describes a non-ergodic state composed by a collection of $\mathcal{N} \sim \exp(r_0^d \ell^d \Sigma(\ell, T))$ metastable states. The free-energy difference between the HOS and the LOS, which, as previously observed, should be purely entropic, in fact coincides with (T times) the configurational entropy in the constrained system, denoted $\ell^d \Sigma(\ell, T)$. In other words there is an exponentially large number \mathcal{N} of metastable states compatible with the boundary condition. The HOS just represents one of them, on the same foot as all the others. The behavior of $\Sigma(\ell, T)$ is depicted in the lower panel of Fig. 0.11, which shows

curves growing with ℓ , crossing the value 0 for $\ell = \ell_c$. If $T > T_d$ the curves stop at the dynamical length ℓ_d beyond which the system recovers ergodicity. For $T < T_d$ the curves tend to the bulk value of the mean-field configurational entropy $\Sigma_\infty(T)$. The dependence of $\Sigma(\ell, T)$ upon ℓ can in both regions be described in a good approximation as $\Sigma(T, \ell) = A(T)(1 - \ell_c/\ell)$, where for $T < T_d$, $A(T) = \Sigma_\infty(T)$. Upon decreasing the values of ℓ towards ℓ_c , the transition to the confined state is driven by the reduction to zero of the configurational entropy. This is decreased by a term that scales as ℓ^{d-1} relative to the total configurational entropy $\ell^d \Sigma(\ell, T)$.

Let us mention without entering in a detailed discussion that in addition to the solutions we discussed, low-overlap RSB solutions with $m \neq 1$ (not respecting the conditional equilibrium conditions) were also found in (58). These represent families of metastable states in the system with free-energy higher than the equilibrium one. For $\ell < \ell_c$ the solution with $m = 1$ gives a negative configurational entropy and is therefore inconsistent. The dominating metastable low overlap state is one of the RSB $m \neq 1$ solutions just mentioned. It has zero configurational entropy and positive energy difference with the HOS.

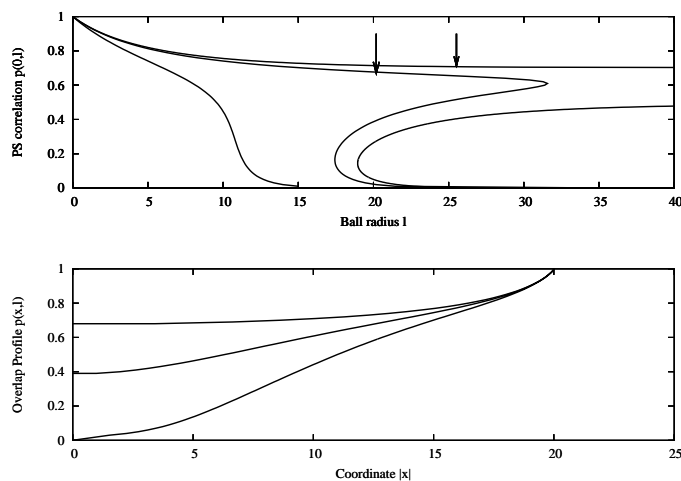


Fig. 0.9 Upper panel: values of the PS function $p(0, \ell)$ for three values of the temperature in the different solutions: $T = 0.676 > T^* = 0.633$, $T = 0.610$, in the interval $[T_d, T^*] = [0.575, 0.633]$ and $T = 0.569$, in the interval $[T_c, T_d] = [0.541, 0.575]$. In the first case there is a unique solution to for all values of ℓ . In the second case three solutions are present for ℓ in the interval $[\ell_0, \ell_d] = [17.31, 31.57]$. In the third case three solutions are present for $\ell > \ell_0 = 19.47$. The arrow mark the points $\ell = \ell_c$. Below ℓ_c the HOS is the thermodynamically favoured state and the LOS is metastable, above that length the roles are interchanged. For the $T = 0.610$, $\ell_c = 20.4$, for $T = 0.569$, $\ell_c = 26.7$. Lower panel: The overlap profiles $p(x; \ell)$ corresponding to the the three solutions for $\ell = 20$ and $T = 0.610$.

The scenario for the various glass transitions as a function of ℓ in the LOS resembles the one of the Mean-Field or diluted p -spin models as a function of temperature.

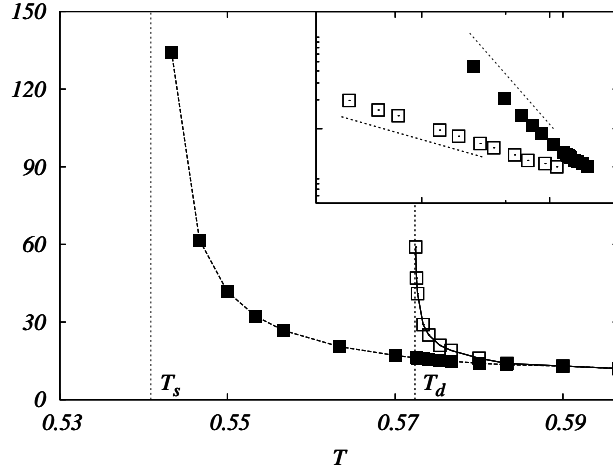


Fig. 0.10 Thermodynamic (filled squares) and dynamic (empty squares) lengths ℓ_c and ℓ_d . The vertical lines correspond to the dynamic and thermodynamic glass transitions $T_c = 0.541847$ and $T_d = 0.57525$. The lengths behave respectively as $\ell_c \sim (T - T_c)^{-1}$ close to T_c and as $\ell_d \sim (T - T_d)^{-1/4}$ close to T_d . In the inset, the lengths as functions of $(T - T_d)$ (for ℓ_d) and $(T - T_c)$ (for ℓ_c). The dotted lines have slope (respectively) $1/4$ and 1 .

We have an ergodic phase for large $\ell > \ell_d$, an intermediate phase with a finite configurational entropy for $\ell_c < \ell < \ell_d$, and a zero configurational entropy 1RSB phase at low $\ell < \ell_c$. We notice that the point at ℓ_d has the character of a typical dynamical transition point of 1RSB systems. This has specific consequences on the dynamical properties (for the constrained dynamics in a ball of radius ℓ) when ℓ gets close to ℓ_d , which should be similar to the one of the mean-field model close to T_d . In particular, for $r_0 \rightarrow \infty$, the relaxation time grows and diverges if the system size goes to ℓ_d from above. On the same foot one can draw consequences on the relaxation time within the metastable states dominating below ℓ_d . One can argue that the stability of these states decreases upon increasing ℓ until they become marginal exactly at ℓ_d (65). Accordingly, the relaxation time within a metastable state diverges if ℓ tends to ℓ_d from below.

As already mentioned the dynamics of the model in the Kac limit is exactly described by inhomogeneous MCT equations (63), so that the bulk relaxation time behaves as $\tau(T) \sim \epsilon^{-\gamma}$ close to T_d , with a model dependent exponent γ (66). For $\ell > \ell_d \sim \epsilon^{-1/4}$ one can expect the scaling

$$\tau(\ell, T) = \frac{1}{\epsilon^\gamma} \hat{\tau}(\ell/\ell_d), \quad (0.44)$$

where the scaling function $\hat{\tau}(u)$ tends to a constant at large arguments, and has a power law behavior $\hat{\tau}(u) \sim (u - 1)^{-\delta}$ for $u \gtrsim 1$. The exponent δ should be in principle derived from the dynamical MCT-like equations (63) and as γ should depend on the choice of the model. An analogous scaling should be expected below ℓ_d with $\tau(\ell, T)$

interpreted as the relaxation time within a state, for the dynamics inside a ball of radius ℓ .

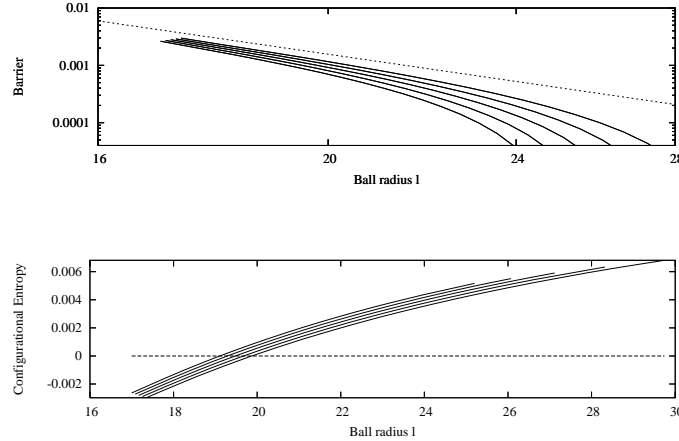


Fig. 0.11 Upper panel: The barrier density as a function of the ball radius ℓ for different temperatures. From bottom to top $T = 0.5819, 0.5816, 0.5812, 0.5809, 0.5805$, all larger than $T_d = 0.57525$. Lower temperatures correspond to higher barriers. The barrier goes to zero for $\ell \rightarrow \ell_d$. The dotted line allows the comparison with the power law ℓ^{-6} expected from scaling close to T_d . Lower panel: Configurational entropy density as a function of ℓ for the same temperatures as in the upper panel. The higher curves correspond to the higher temperatures. The configurational entropy curves touch zero at the mosaic length ℓ_c and terminate at the dynamical length ℓ_d . Both lengths increase for decreasing temperatures. Below the length ℓ_d the correct solution should include RSB.

The thermodynamic mosaic length ℓ_c , whose temperature behavior is shown in Fig. 0.10, displays no singularity at T_d . This is coherent with the fact that for any finite r_0 the dynamical transition is rounded-off and the relaxation time remains finite, and is in agreement with the inequalities (0.8) of Sec. 0.2.3. Its behavior becomes singular near the ideal glass transition point $T \gtrsim T_c$. Here the two minima of V are almost degenerate, and ℓ_s is large. The solutions of the field equations in spherical geometry for $d > 1$ can be obtained through the “thin wall approximation” of nucleation theory (67). This self-consistently neglects the thickness of the interface region, where the solution passes from values of p close to q_{EA} to values close to zero, this thickness being small with respect to ℓ_c . Let us consider $\ell \gtrsim \ell_c$. The transition is driven by a bulk contribution to the configurational entropy $\Sigma_\infty(T)\ell^d$ and an almost temperature independent surface entropy reduction $-Y\ell^{d-1}$. The value of Y can be computed in analogy with standard nucleation theory as the action of the “instantonic solution” to the field equation that connects the two degenerate minima of $V(p)$ at $T = T_c$:

$$Y = S_d \int_0^{q_{EA}} dp \frac{2V(p)}{\sqrt{\frac{c}{2}\beta\phi''(p)V(p)}} \Big|_{T=T_c}, \quad (0.45)$$

where S_d is the surface of the unitary sphere in dimension d , $S_d = 2\pi^{d/2}\Gamma(d/2)$. The length ℓ_c is then found from the cancellation of the total configuration entropy,

$$\ell^d \Sigma(\ell, T) = \Sigma_\infty(T) \ell^d - Y \ell^{d-1}, \quad (0.46)$$

namely $\ell_c = Y/\Sigma_\infty(T)$. The length ℓ_c diverges at T_c , with the scaling

$$\ell_c \sim \frac{Y}{\Sigma_\infty(T)} \sim \frac{Y}{T - T_c}. \quad (0.47)$$

We will see in the next sub-section that this is also the typical spatial extension of barrier states close to T_c . Notice that the negative contribution to (0.46) is proportional to the ball surface. As we discuss in sec. 0.4.3 phenomenological theories (1; 9) suggest that interface reduction terms could scale as ℓ^θ with $\theta < d - 1$. As all qualitative results we present the value $\theta = d - 1$ can be checked to be independent on the choice of the model in the 1RSB class or the various approximations like the thin wall approximation or the gradient expansion of the interaction that we have used to simplify the analytic treatment. Our derivation, however, depends crucially on the Kac limit, that in our analysis precedes the limit $T \rightarrow T_c$. It is certainly possible that for finite r_0 a non trivial cross-over could change this exponent.

The barrier state. Let us complete our analysis with a discussion of the medium overlap solution (MOS). In figures 0.9 the value of $p(0; \ell)$ plotted in the MOS has been obtained supposing conditional equilibrium as an approximation. Unfortunately, it is difficult to go beyond this solution using numerical integration. Since by definition the MOS is an unstable saddle of W , iterative methods that work well for minima, simply do not find the solution. Experience with the replica method shows however that such replica symmetric solutions often give good approximations for the free-energy and other quantities even in regions where the exact description should include RSB.

We analyze below the regimes of temperatures close to T_d and T_c where scaling can be expected and analytic arguments allow to go beyond numerical integration of the field equations. We believe that our approximate solution while possibly failing in numeric prefactors, gives back the correct scaling behavior describing the dependence of the MOS on system size and temperature for large r_0 .

The MOS is interpreted physically as a dynamical barrier state to be overcome during relaxation (68). The equilibrium activation barrier $\mathcal{B}(\ell, T)$ can be estimated as the free-energy difference between the MOS and the HOS

$$r_0^d \mathcal{B}(\ell, T) = W_{MOS} - W_{HOS}. \quad (0.48)$$

This is, for all temperatures, a decreasing function of the system size ℓ . For temperatures in the range $[T_d, T^*]$ the barrier vanishes at ℓ_d , coherently activation is not needed for relaxation in large systems. For temperatures below T_d activation is required at all scales. The barrier for bulk relaxation can be obtained as the large ℓ limit of $\mathcal{B}(\ell, T)$.

Close to T_d the behavior of the MOS and the HOS become independent of the details of the model. Since we do not expect RSB to affect the scaling, we can obtain the behavior of the various quantities through dimensional analysis of the cubic field theory of Eq. (0.43). The main results of this analysis are that

- For $T \gtrsim T_d$ the barrier is non zero for $\ell < \ell_d$ and admits the scaling form

$$\mathcal{B}(\ell, T) = \ell^{d-6} b_+(\ell/\ell_d) , \quad (0.49)$$

where the scaling function is such that the barrier vanishes linearly as $\ell \rightarrow \ell_d$: $b_+(x) \approx \text{Const.} \times (1-x)$ for $x \rightarrow 1$ and $b_+(x) = 0$ for $x > 1$. The behavior of the barrier in this region is shown in the upper panel of fig. 0.11.

- For $T \lesssim T_d$ the barrier admits the scaling form

$$\mathcal{B}(\ell, T) = |\epsilon|^{\frac{6-d}{4}} b_-(\ell|\epsilon|^{1/4}) , \quad (0.50)$$

where the function $b_-(x)$ is a decreasing function of x that admit a positive limit for $x \rightarrow \infty$. As already noticed, from (0.50) we can obtain the barrier for relaxation in the bulk as the limit of large ℓ of $\mathcal{B}(\ell, T)$. This coincides with a direct estimate of the barrier in (61; 69) where boundary conditions are imposed at infinity and scales as $\mathcal{B}_\infty(T) \sim |\epsilon|^{\frac{6-d}{4}}$. The scaling (0.50) shows that the asymptotic value is reached on lengths of order $\ell_b \sim |\epsilon|^{-1/4}$. This is then the typical spatial extension of dominating barrier modes governing the relaxation in the bulk, which becomes large on approaching T_d from below.

Let us now turn to temperatures close to the static transition temperature T_c . Analogously to the case of the equilibrium solutions of the previous subsection, for small $T - T_c$ nucleation arguments can be used to study the barrier. For large ℓ , the barrier solution $p(x; \ell)$ has the shape of a bubble of small overlap values in a sea where $q(x; \ell) \approx q_{EA}$. This is surrounded by a crown around the boundary of \bar{B} where p decays from 1 to $\approx q_{EA}$. For $d > 1$ the typical bubble radius ℓ_b , and the barrier value can be just estimated from the point of maximum of expression (0.46)⁴. This gives, as announced, a common scaling for ℓ_b and ℓ_c ,

$$\ell_b \sim \frac{Y}{\Sigma_\infty(T)} \sim (T - T_c)^{-1} , \quad (0.51)$$

and for the barrier the behavior

$$\mathcal{B}(\ell, T) \sim Y^d (\Sigma_\infty(T))^{-(d-1)} \sim (T - T_c)^{-(d-1)} , \quad (0.52)$$

which is divergent for $d > 1$ when $T \rightarrow T_c$. Eq. (0.52) has the form of a modified Adams-Gibbs inverse proportionality relation between the relaxation barrier and the configurational entropy(70). In turn, using $\Sigma_\infty(T) \sim T - T_c$, one finds a modified Vogel-Fulcher law⁵ with an exponent that depends on dimensionality, with associated lower critical dimension $d_{LCD} = 1$. We remark the coincidence of this result in the Kac limit with the naive analysis of (1). The comment we made at the end of section (0.4.3) on the exponent can be verbatim applied here to the modified Vogel-Fulcher exponent.

⁴The 1d case requires a special analysis and one finds that $\ell_b \sim -\log(T - T_c)$.

⁵The usual Vogel-Fulcher form posits a barrier proportional to $(T - T_c)^{-1}$.

Correlations in wall geometry. Before concluding our discussion on the Kac limit, let's have a closer look to the three solutions for large $\ell \gg \ell_c$ and $T \gtrsim T_c$. The large ℓ limit is equivalent to imposing the boundary condition on a single planar wall. This condition has been object of recent numerical experiments (18) and deserves a short comment.

The question here is up to which distance the boundary has an effect on the configuration of the system, i.e. what is the typical distance from the boundary over which $p(x; \ell)$ decays to zero and if this distance coincides with ℓ_c . The behavior of the three solutions in this regime can be easily worked out from the field equation. The metastable HOS never loses correlations: after a rapid decay from 1 on the wall, which is common with the MOS and the LOS, stabilizes to $p(x; \ell) \simeq q_{EA}$. The unstable MOS persists to values $p(x; \ell) \approx q_{EA}$ up to distances of order ℓ from the wall. It decays to zero at a distance ℓ_c from the center and is similar to a ball of radius ℓ_c of small overlap in a sea of large overlap values. More interesting is the behavior of the LOS which gives the equilibrium profile. In this case the overlap decays to low values over distances of order of a "wetting" length $\ell_w \sim -\log(T - T_c)$ from the boundary before decaying to values close to zero. We conclude that the semi-infinite wall geometry fails to identify the correlations ℓ_c while it identifies a much smaller length ℓ_w .

Beyond the Kac limit. The results presented so far are strictly valid in the Kac limit. We briefly discuss here some possible scenarios for r_0 large but finite.

We would like first to discuss the rounding off of the dynamical (MCT) transition. The analysis can be performed in analogy with ferromagnetic models with Kac interactions below the lower critical dimension where "finite range scaling" (FRS) holds (71). The basic hypothesis of FRS is that the interaction range acts as a cut-off to critical behavior in a similar way as finite size does for usual critical phenomena. This idea has been employed in a 1d Kac spin glass with a continuous transition in the Kac limit, to predict the rate of growth of the correlation length with r_0 at the mean-field critical temperature of the model (72). The $r_0 \rightarrow \infty$ dynamical critical point has a mean-field character, so that one can expect mean-field scaling. An observable O which depends on T , r_0 and ℓ , should be described by scaling as:

$$O(T, r_0, \ell) = \epsilon^{-y_0} \hat{O}(r_0^a \epsilon^{1/4}, \ell \epsilon^{1/4}) . \quad (0.53)$$

The scaling function \hat{O} is such to cut-off both the singularity that appear for $r_0 \rightarrow \infty$ at $\ell = \ell_d$ for $\epsilon > 0$ and the one at $\ell \rightarrow \infty$ and $\epsilon = 0$. The value of the exponent a could be guessed if one used the potential functional as an ordinary field theory beyond the Kac limit for which it has been derived. Simple rescaling of the cubic action (0.43) leads then to $a = \frac{d}{6-d}$, implying that the cross-over from Mean-Field MCT behavior to non-critical behavior happens on length scales of the order of $\ell_1 = r_0^{\frac{d}{6-d}}$. The same conclusion could be reached analysing the behavior of the barrier for $T \lesssim T_d$ and $\ell \lesssim \ell_d$, which scales as $r_0^d \mathcal{B}(\ell, T) \sim r_0^d \ell^{d-6} (1 - \ell/\ell_d)$. This analysis, however, relies on a continuum approximation of the potential $W[p(x)]$, which for finite r_0 neglects spatial fluctuations of the quenched disorder and heterogeneities in the reference configuration $\underline{\sigma}^{(0)}$. It has been recently observed that finite size scaling around mean-field critical points in disordered systems can be non-trivial due to effective fluctuations of

the critical temperature (73; 74). Analogously here we can expect that effective local fluctuations of the critical temperatures can affect FRS. A criterion for the validity of naive FRS can be obtained in analogy with the analysis of FSS in disordered systems which in turn is an application of Harris criterion (75) for relevance of disorder in phase transitions.

Let us rewrite the naive FRS of the barrier for temperatures slightly smaller than T_d , which for $\ell \rightarrow \infty$ we write as

$$r_0^d \mathcal{B}_\infty(T) \sim r_0^d |\epsilon|^{\nu_{MF}(d_c-d)} \quad (0.54)$$

In our case, $\nu_{MF} = 1/4$ and $d_c = 6$; the form (0.54) offers the possibility of studying more general cases. The scaling (0.54) gives a characteristic cross-over length $\ell_1 \sim r_0^{\frac{d}{d_c-d}}$ beyond which deviations from mean-field theory are to be expected (remember that lengths are measured in units of r_0). One can expect violations of this naive FRS when, on scale ℓ_1 the typical fluctuations of the critical temperature are larger than the average deviation $|\epsilon|$. The critical temperature fluctuations, related to local disorder fluctuations, can be expected to be of the order $(r_0 \ell_1)^{-d/2}$. Applying the above criterion, we find that naive FRS is violated if $r_0^{-\left(\frac{d}{(d_c-d)\nu_{MF}}\right)} \ll r_0^{-\frac{d}{2}\frac{d_c}{(d_c-d)}}$ i.e. if $d_c \nu_{MF} < 2$. It is notable that this relation coincides with the criterion for the validity of naive FSS for disordered systems above the upper critical dimension. In our case $d_c \nu_{MF} = 3/2$ and so that naive scaling cannot not be expected to hold. In order to understand the nature of the cross-over for finite r_0 a deep analysis of the effect of critical temperature fluctuations is needed (74). This goes beyond the scope of the present review and won't be attempted here.

The second point we would like to discuss is the behavior of the barrier close to T_c . The Kac limit prediction is that the configurational entropy reduction in a finite volume of linear size $\ell > \ell_c$ is proportional to the surface, $\delta\Sigma \ell^d = -Y \ell^{d-1}$, which, as observed, leads to a modified Vogel-Fulcher law for the relaxation time $\tau \sim \exp(r_0^d (T - T_c)^{-(d-1)})$. Of course this does not necessarily imply an ideal glass transition if r_0 is finite. It just tells that for growing r_0 and fixed temperature $T \leq T_c$ the relaxation time grows faster than $\exp(r_0^d \mathcal{B})$ for any $\mathcal{B} > 0$. The result is compatible both with the absence of a singularity at finite temperature or with a singularity that could be weaker than the one found in the Kac limit. In phenomenological RFOT it is supposed that the interface exponent is renormalized by the effect of fluctuations, yielding $\delta\Sigma \ell^d = -Y \ell^\theta$ with $\theta \leq d - 1$. In ref. (1), scaling arguments in favor of the value $\theta = d/2$ have been put forward, which leads to the canonical Vogel-Fulcher form in all dimensions $d \geq 2$. Correspondingly, the static length ℓ_c would behave as $(T - T_c)^{-d/2}$ rather than $(T - T_c)^{-1}$ as found for $r_0 \rightarrow \infty$. If these suggestions are correct, for large but finite r_0 there should be a cross-over between the two regimes. A Ginzburg criterion involving r_0 as well as $T - T_c$ should govern this cross-over⁶. Differently from the cross-over close to T_d the formalism we have used does not seem to suggest a mechanism for this cut-off.

⁶Note that if we ask here that the fluctuations of the critical temperature on a correlated volume are smaller than $T - T_c$ we get the condition $(T - T_c) \gg \frac{1}{(r_0 \ell_c)^{d/2}}$ which is always verified for $\ell_c \sim (T - T_c)^{-1}$.

0.5 Conclusions

This chapter concerns the inclusion of spatial aspects in glassy theory. In particular the emphasis has been put on recently proposed measures of correlations -the point-to-set correlations- that involve an infinite number of variables.

In the first part of the chapter we reviewed exact general bounds that relate the growth of a relaxation time to the growth of a correlation length. We first introduced with a progressive mathematical rigor the idea of point-to-set correlation functions and the associated correlation lengths, and explained to which extent this definition allows to reconcile the phenomenology of glasses with the intuitive association between growing time and length scales. These bounds do not spoil the interest of studying PS correlations in glassy systems. The lower and upper bounds have different forms, which correspond to different physical mechanisms of relaxation. The lower-bound is, up to a non-trivial exponent, of the critical dynamics type, while the upper-bound has the form of activated dynamics.

In the second part of this chapter we discussed this correlation length in the context of the mean-field picture of glassy phenomena provided by 1RSB disordered models. We have thus reviewed some analytical works dedicated to growing length scales in simplified models of glasses and their puzzling relationship with growing time scales. We discussed diluted random graph models and Kac like models which add new elements to the already rich behaviour of fully-connected models of the p -spin family. For random graph models we found that the divergence of the point-to-set length accompanies the one of the relaxation time at the dynamical transition.

The study of the Kac model reveals a rich scenario with two relevant correlation lengths, the mosaic length below which a system behaves thermodynamically as an ideal glass, and a dynamical length quantifying the typical extension of relaxation modes which do not require activation. At the dynamical transition the former remain finite, coherently with the fact that for any finite interaction range the transition is rounded-off, while the latter diverges.

Let us close this discussion with a few open questions.

The upper bound in Eq. (0.8) implies that the divergence of the equilibrium correlation time is necessarily accompanied by a divergence of the point-to-set correlation length, even though with a possibly much slower form of the divergence. Both in diluted random graph models, and in spin models in the Kac limit, the divergence of the point-to-set correlation length at T_d cannot be detected by the study of static n -point correlation function, for any finite n . Hence in these models there is a true separation between the dynamic transition and the thermodynamic one, the free-energy having a singularity only at a lower temperature T_c . An important open question is to determine whether this phenomenon of growth of the point-to-set correlation function without a trace in the two-point function can persist in finite-dimensional models or if this is an artifact of mean-field models. In the latter case it would mean that bounds of the form (0.8) holds with ℓ being replaced by a standard two-point correlation length (and different constants $C_{1,2}$). This should be important from a theoretical point of view, yet would not contradict the experimental and numerical situation. On the range of correlation time where measurements are possible the growth of the static correlations implied by this hypothetical extension of (0.8) could still be very weak.

Other questions relate to the study of finite range disordered models beyond the Kac limit. An accomplished theory of finite range scaling close to the dynamical temperature T_d should enable to theoretically describe the crossover between mode coupling regime to activated dynamics. A related question is the connection between the purely static correlation length discussed here and the dynamical one extracted from four-points (two-time, two-location) dynamical susceptibilities. As we have discussed, the dynamical length found in MCT above T_d can be detected in the Kac limit analyzing metastable solutions of the field equations in finite geometry. In this case, dynamic and static correlation length do not coincide. It would be important to better understand the quantitative relationship between these two characterizations of the correlations in a system.

Acknowledgments

We warmly thank Andrea Montanari, Giorgio Parisi and Fabio-Lucio Toninelli for fruitful collaborations on several works presented here.

References

- (1) T.R. Kirkpatrick and P.G. Wolynes, *Phys. Rev. B* **36**, 8552 (1987), T. R. Kirkpatrick, D. Thirumalai and P.G. Wolynes, *Phys. Rev. A* **40**, 1045 (1989).
- (2) M. Mézard, G. Parisi and M.A. Virasoro, *Spin glass theory and beyond*, World Scientific, Singapore (1987).
- (3) F. Sciortino and P. Tartaglia, *Phys. Rev. Lett.* **86**, 107 (2001).
- (4) L. Berthier, G. Biroli, J.-P. Bouchaud, L. Cipelletti, D. El Masri, D. L'Hôte, F. Ladieu and M. Pierno, *Science* **310**, 1797 (2005).
- (5) M. Mézard and G. Parisi, *Phys. Rev. Lett.* **82**, 747 (1999), *J. Phys. Condens. Matter A* **11**, 157 (1999), G.Parisi and F.Zamponi, *J. Stat. Mech.* P03026 (2009).
- (6) C. Donati, J. F. Douglas, W. Kob, S. J. Plimpton, P. H. Poole and S. C. Glotzer, *Phys. Rev. Lett.* **80** 2338 (1998).
- (7) C. Donati, S. Franz, S. C. Glotzer and G. Parisi, *J. Non-Cryst. Solids* **307**, 215 (2002), S. Franz and G. Parisi, *J. Phys.: Condens. Matter* **12**, 6335 (2000).
- (8) G. Biroli and J.-P. Bouchaud, *Europhys. Lett.* **67**, 21 (2004).
- (9) G. Biroli and J.-P. Bouchaud, *J. Chem. Phys.* **121**, 7347 (2004).
- (10) A. Montanari and G. Semerjian, *J. Stat. Phys.* **125**, 23 (2006).
- (11) E. Mossel, *Survey: Information flow on trees*, in *Graphs, Morphisms and Statistical Physics*, DIMACS series in discrete mathematics and theoretical computer science, J. Nestril and P. Winkler eds. 155, [arXiv:math/0406446](https://arxiv.org/abs/math/0406446) (2004).
- (12) F. Martinelli, A. Sinclair and D. Weitz, *Comm. Math. Phys.* **250**, 301 (2004).
- (13) F. Kschischang, B.J. Frey and H.-A. Loeliger, *IEEE Transactions on Information Theory* **47**, 498 (2001).
- (14) E. Zarinelli and S. Franz, *J. Stat. Mech.* (2010) P04008
- (15) A. Cavagna, T.S. Grigera and P. Verrocchio, *Phys. Rev. Lett.* **98**, 187801 (2007).
- (16) G.H. Fredrickson and H.C. Andersen, *Phys. Rev. Lett.* **53**, 1244 (1984).
- (17) W. Kob and H.C. Andersen, *Phys. Rev. E* **48**, 4364 (1993).
- (18) P. Scheidler, W. Kob and K. Binder, *Europhys. Lett.* **52**, 277 (2000), P. Scheidler, W. Kob, K. Binder and G. Parisi, *Phil. Mag. B* **82**, 283 (2002), P. Scheidler, W. Kob and K. Binder, *J. Phys. Chem. B* **108**, 6673 (2004).
- (19) R.L. Jack and J.P. Garrahan, *J. Chem. Phys.* **123**, 164508 (2005).
- (20) C. Cammarota, A. Cavagna, G. Gradenigo, T.S. Grigera and P. Verrocchio, [arXiv:0906.3868](https://arxiv.org/abs/0906.3868) (2009).
- (21) G. Biroli, J.-P. Bouchaud, A. Cavagna, T.S. Grigera and P. Verrocchio, *Nature Phys.* **4**, 771 (2008).
- (22) T. Lindvall, *Lectures on the Coupling Method*, Dover Publications (2002).
- (23) J. van den Berg, *Comm. Math. Phys.* **152**, 161 (1993).
- (24) T.P. Hayes and A. Sinclair, *Ann. Appl. Probab.* **17**, 931 (2007).

- (25) G. Parisi, *Glasses, Replicas and all that*, Les Houches summer school LXXVII, 271 (2002).
- (26) L.F. Cugliandolo, *Dynamics of glassy systems*, Les Houches summer school LXXVII, 367 (2002).
- (27) T. Castellani and A. Cavagna, *J. Stat. Mech.* P05012 (2005).
- (28) L. Viana and A.J. Bray, *J. Phys. C: Solid State Phys.* **18**, 3037 (1985).
- (29) M. Mézard and A. Montanari, *Information, Physics and Computation*, Oxford University Press (2009).
- (30) M. Mézard, F. Ricci-Tersenghi and R. Zecchina, *J. Stat. Phys.* **111**, 505 (2003).
- (31) S. Cocco, O. Dubois, J. Mandler and R. Monasson, *Phys. Rev. Lett.* **90**, 047205 (2003).
- (32) M. Mézard and G. Parisi, *Eur. Phys. J. B* **20**, 217 (2001).
- (33) R. Monasson, *J. Phys. A* **31**, 515 (1998).
- (34) A. Montanari and G. Semerjian, *J. Stat. Phys.* **124**, 103 (2006).
- (35) J. Vannimenus, *Z. Phys. B* **43**, 141 (1981).
- (36) J.P. Straley, *J. Phys. C: Solid State Phys.* **15**, 2333 (1982).
- (37) A. Barrat and R. Zecchina, *Phys. Rev. E* **59**, R1299 (1999).
- (38) A. Montanari and F. Ricci-Tersenghi, *Phys. Rev. B* **70**, 134406 (2004).
- (39) J.-P. Bouchaud, L.F. Cugliandolo, J. Kurchan and M. Mézard, *Physica A* **226**, 243 (1996).
- (40) M. Mézard and A. Montanari, *J. Stat. Phys* **124**, 1317 (2006).
- (41) A. Montanari, F. Ricci-Tersenghi and G. Semerjian, *J. Stat. Mech.* P04004 (2008).
- (42) M. Kac, *Phys. Fluids* **2**, 8 (1959).
- (43) J. L. Lebowitz and O. Penrose, *J. Math. Phys.* **7**, 98 (1966).
- (44) J. L. Lebowitz and O. Penrose, *J Stat. Phys.* **3**, 211 (1971).
- (45) A Bovier, *J. Stat. Phys.* **91**, 459 (1998).
- (46) J.L. Lebowitz, A.E. Mazel and E. Presutti, *Phys. Rev. Lett.* **80**, 4701 (1998).
- (47) J. Froehlich and B. Zegarlinski , *Commun. Math. Phys.* **112**, 553 (1987).
- (48) S. Franz and F.L. Toninelli, *J. Phys. A* **37**, 7433 (2004).
- (49) P.A. Vuillermot, *J. Phys. A* **10**, 1319 (1977).
- (50) S. Franz and F.L. Toninelli, *Phys. Rev. Lett.* **92**, 030602 (2004).
- (51) J. Kurchan, G.Parisi and M.A. Virasoro, *J. Phys. I (France)* **3**, 1819 (1993).
- (52) S. Franz and G. Parisi, *J. Phys. I (France)* **5**, 1401 (1995), *Phys. Rev. Lett.* **79** 2486 (1997), *Physica A* **261**, 317 (1998).
- (53) E. Marinari, G. Parisi, F. Ricci-Tersenghi, J. J. Ruiz-Lorenzo and F. Zuliani, *J. Stat. Phys.* **98**, 973 (2000).
- (54) S. Franz, M. Mezard, G. Parisi and L. Peliti, *J. Stat. Phys.* **97**, 459 (1999).
- (55) F. Guerra and F. L. Toninelli , *Commun. Math. Phys.* **230**, 71 (2002).
- (56) F. Guerra , *Commun. Math. Phys.* **233**, 1 (2003).
- (57) M. Talagrand, *C. R. Acad. Sci. Paris, Ser. I* **337**, 111 (2003).
- (58) S. Franz and A. Montanari, *J. Phys. A* **40**, F251 (2007).
- (59) G. Alberti, G. Bellettini, M. Cassandro and E. Presutti, *J. Stat. Phys.* **82**, 743 (1996).
- (60) S. Franz and F.L. Toninelli, *J. Stat. Mech.* P01008 (2005).

- (61) S. Franz, J. Stat. Mech. P04001 (2005).
- (62) R. Monasson, Phys. Rev. Lett. **75**, 2847 (1995).
- (63) S. Franz, J. Stat. Phys. **126**, 765 (2007).
- (64) C. B. Muratov and E. Vanden-Eijnden, J. Stat. Phys. **114**, 605 (2004).
- (65) A. Barrat, *The p-spin spherical spin glass model*, arXiv:cond-mat/9701031, unpublished.
- (66) Recent reviews on MCT can be found in D. R. Reichman and P. Charbonneau, J. Stat. Mech. P05013 (2005), and S. Das, Rev. Mod. Phys. **76**, 785 (2004).
- (67) J.S. Langer, Ann. Phys. **41**, 108 (1967), Ann. Phys. **54**, 258 (1969).
- (68) S. Franz, Europhys. Lett. **73**, 492 (2006).
- (69) M. Dzero, J. Schmalian and P. G. Wolynes, Phys. Rev. B **72**, 100201 (2005).
- (70) G. Adams and J.-H. Gibbs, J. Chem. Phys., 43 (1965) 139.
- (71) A. Pelissetto and E. Vicari, Phys. Rep. **368**, 549 (2002), E. Luijten and K. Binder, Phys. Rev. E **58**, 4060 (1998).
- (72) S. Franz and G. Parisi, Europhys. Lett. **75**, 385 (2006).
- (73) T. Sarlat, A. Billoire, G. Biroli and J.-P. Bouchaud, J. Stat. Mech. P08014 (2009).
- (74) Silvio Franz, Giorgio Parisi, Federico Ricci-Tersenghi, Tommaso Rizzo *Properties of the perturbative expansion around the mode-coupling dynamical transition in glasses* preprint arXiv:1001.1746
- (75) A.B. Harris, J. Phys. C **7**, 1671 (1974)